

Electronic Supplementary Information for

**Dinitrogen-derived (diarylboryl)diazenido Complexes with Differing
Coordination to the Thallium Cation**

Amal Bouammali, Anaïs Coffinet, Laure Vendier and Antoine Simonneau*

*LCC-CNRS, Université de Toulouse, CNRS, UPS, 205 route de Narbonne, BP44099, F-31077 Toulouse
cedex 4, France.*

E-mail:

antoine.simonneau@lcc-toulouse.fr

TABLE OF CONTENTS

I. GENERAL INFORMATION.....	3
II. SYNTHESSES AND CHARACTERIZATION OF NEW COMPOUNDS.....	3
II.1. Synthesis and characterization of the complex $[W(Cl)\{N_2BMes_2\}(dppe)_2]$ (2^{Ph}).....	3
II.2. General procedure for the synthesis of complexes $[W(Cl)\{N_2B(Ar)_2\}\{R_2P(CH_2)_2PR_2\}_2]$ ($\{Ar,R\} = \{Mes,Et\}, 2^{Et}; \{Ar,R\} = \{C_6F_5,Ph\}, 3^{Ph}; \{Ar,R\} = \{C_6F_5,Et\}, 3^{Et}$).....	4
II.3. Characterization of the complexes $[W(Cl)\{N_2B(Ar)_2\}\{R_2P(CH_2)_2PR_2\}_2]$ ($\{Ar,R\} = \{Mes,Et\}, 2^{Et}; \{Ar,R\} = \{C_6F_5,Ph\}, 3^{Ph}; \{Ar,R\} = \{C_6F_5,Et\}, 3^{Et}$).....	4
II.3.1 $[W(Cl)\{N_2BMes_2\}(depe)_2]$ (2^{Et}).....	4
II.3.2 $[W(Cl)\{N_2B(C_6F_5)_2\}(dppe)_2]$ (3^{Ph}).....	4
II.3.1 $[W(Cl)\{N_2B(C_6F_5)_2\}(depe)_2]$ (3^{Et}).....	4
II.4. General procedure for the reaction of compounds 2^{Et} , 3^{Ph} and 3^{Et} with $TIBArF_4$	5
II.5. Characterization of the complexes $[Ti(W\{Cl\}\{N_2B(R)_2\}\{L\}_2)]BARF_4$ ($\{R,L\} = \{Mes,depe\}$ or $\{C_6F_5,dppe\}$) ($[2^{Et}\cdot Ti]BARF_4$ and $[3^{Ph}\cdot Ti]BARF_4$).....	5
II.5.1 $[W(Cl)(NN(Ti)\{B(Mes)_2\})(depe)_2]BARF_4$ ($[2^{Et}\cdot Ti]BARF_4$).....	5
II.5.2 $[W(ClTi)\{N_2B(C_6F_5)_2\}(dppe)_2]BARF_4$ ($[3^{Ph}\cdot Ti]BARF_4$).....	5
III. SPECTROSCOPIC DATA OF NEW COMPOUNDS	7
III.1. $[W(Cl)\{N_2BMes_2\}(dppe)_2]$ (2^{Ph}) in the reaction mixture.....	7
III.2. $[W(Cl)\{N_2BMes_2\}(depe)_2]$ (2^{Et}).....	12
III.3. $[W(Cl)\{N_2B(C_6F_5)_2\}(dppe)_2]$ (3^{Ph}).....	17
III.4. $[W(Cl)\{N_2B(C_6F_5)_2\}(depe)_2]$ (3^{Et}).....	22
III.1. $[W(Cl)(NN(Ti)\{B(Mes)_2\})(depe)_2]$ ($[2^{Et}\cdot Ti]BARF_4$).....	27
III.2. $[W(ClTi)\{N_2B(C_6F_5)_2\}(dppe)_2]$ ($[3^{Ph}\cdot Ti]BARF_4$).....	33
IV. CRYSTALLOGRAPHIC DATA.....	40
IV.1. Data collection and refinement.....	40
IV.1. X-Ray analysis of 2^{Ph}	41
IV.2. X-Ray analysis of 2^{Et}	42
IV.3. X-Ray analysis of 3^{Ph}	43
IV.4. X-Ray analysis of 3^{Et}	44
IV.5. X-Ray analysis of $[WCl_2(depe)_2]BARF_4$	45
IV.6. X-Ray analysis of $[3^{Ph}\cdot Ti]BARF_4$	46
IV.7. X-Ray analysis of $[2^{Et}\cdot Ti]BARF_4$	47
V. REFERENCES.....	48

I. General Information

All manipulations were carried out under a dry and oxygen free argon or dinitrogen atmosphere using Schlenk techniques and a Jacomex glove box. The water and oxygen levels were kept at less than 1.0 ppm and 0.5 ppm respectively. Glassware was oven- or flame-dried before use. Solvents were pre-dried (toluene and *n*-pentane by passing through a Puresolv MD 7 solvent purification machine), degassed by freeze-pump-thaw cycles, dried with molecular sieves and stored in the glove box. C₆D₆ and C₆D₅Cl (purchased from Eurisotop) was degassed by freeze-pump-thaw cycles, dried with molecular sieves and stored in the glove box. ¹H, ¹³C, ¹¹B, ¹⁹F, and ³¹P NMR spectra were recorded in C₆D₆ or C₆D₅Cl using NMR tubes equipped with J. Young valves on a Bruker Avance III 400 spectrometer. Chemical shifts are reported in parts per million (ppm) downfield from tetramethylsilane and were referenced to the residual solvent resonance as the internal standard for ¹H and ¹³C NMR experiments. ¹¹B and ³¹P NMR spectra were calibrated according to the IUPAC recommendation.^{S1} Data are reported as follows: chemical shift, multiplicity (br = broad, s = singlet, d = doublet, t = triplet, q = quartet, quint = quintet, m = multiplet), coupling constant (Hz), assignment and integration. Infrared (IR) spectra were recorded in the glove box on an Agilent Cary 630 FT-IR spectrophotometer equipped with ATR or transmission modules and are reported in wavenumbers (cm⁻¹) with (s) indicating strong absorption. Elemental analyses were performed on samples sealed in tin capsules under dinitrogen by the Analytical Service of the Laboratoire de Chimie de Coordination; results are the average of two independent measurements. *trans*-[W(L)₂(N₂)₂] (L = dppe, **1**^{Ph};S² L = depe, **1**^{EtS³), B(Cl)(R)₂ (R = C₆F₅,^{S4} mesityl {Mes}^{S5}) and TIBAr^F₄ (Ar^F = 3,5-(CF₃)₂C₆H₃)^{S6} were prepared according to reported procedures. Unless otherwise noted, other reagents were purchased from commercial suppliers and used without further purification.}

II. Syntheses and Characterization of New Compounds

II.1. Synthesis and characterization of the complex [W(Cl){N₂BMes₂}(dppe)₂] (**2**^{Ph})

In a glove box, the dinitrogen complex *trans*-[W(dppe)₂(N₂)₂] (**1**^{Ph}, 31 mg, 30 μmol) was weighed in a 4-mL glass vial and dissolved in C₆D₆ (0.5 mL). Dimesityl(chloro)borane (26 mg, 90 μmol, 3 equiv) was added at room temperature to the orange C₆D₆ solution of **1**^{Ph} in one portion. The mixture was then transferred to an NMR tube equipped with a J. Young valve and was irradiated at 365 nm for 18 days. A conversion of ca. 40% to the boryldiazenido-chloro complex was recorded according to ³¹P NMR analysis. Single crystals spontaneously grew in the NMR tube upon standing at room temperature for a few days. They were recovered by decantation and submitted to X-ray diffraction and IR spectroscopy analyses.

Yellow crystals, isolated yield 30% (11 mg, 9 μmol). The collected amount of crystals were not sufficient to perform other analyses than X-ray diffraction and IR spectroscopy; NMR spectra were recorded from the crude mixture that contains **1**^{Ph} and B(Cl)Mes₂. **¹H NMR** (400 MHz, C₆D₆) δ = 7.55–7.44 (m, 8H, **Ar**), 7.25–7.15 (m, overlaps with signals of **1**^{Ph}, 12 H, **Ar**), 6.92 (t, *J* = 7.2 Hz, 4H, **Ar**), 6.89–6.81 (m, 16H, **Ar**), 6.79 (s, overlaps with signals of B(Cl)Mes₂, *m*-**Ar**, 4H), 2.70–2.53 (m, 8H, P-CH₂-CH₂-P), 2.25 (s, 6H, *p*-Ar-CH₃), 1.97 (s, 12H, *o*-Ar-CH₃). **¹¹B NMR** (128 MHz, C₆D₆) δ = 70.7 (B(Cl)Mes₂). **¹³C NMR** (101 MHz, C₆D₆) δ = 134.0 (td, *J* = 38.1, 4.9 Hz, **Ar**), 133.1–132.5 (m, *o*-Ar^{Mes}), 129.1 (s, *p*-Ar^{Mes}), 30.6–29.9

(m, P-CH₂-CH₂-P), 22.9 (s, *p*-Ar-CH₃), 21.1 (s *o*-Ar-CH₃). ³¹P{¹H} NMR (162 MHz, C₆D₆) δ 37.2 (¹J_{WP} = 292.8 Hz). IR (ATR) ν/cm⁻¹ = 3054, 2916, 1948, 1602, 1433, 1395, 1235, 1197, 1093, 846, 809, 742.

II.2. General procedure for the synthesis of complexes [W(Cl){N₂B(Ar)₂}{R₂P(CH₂)₂PR₂}] ({Ar,R} = {Mes,Et}, 2^{Et}; {Ar,R} = {C₆F₅,Ph}, 3^{Ph}; {Ar,R} = {C₆F₅,Et}, 3^{Et}).

In a glove box, the dinitrogen complex *trans*-[W{R₂P(CH₂)₂PR₂}]₂(N₂)₂ (**1**^R with R = Ph or Et, 30 μmol) is weighed in a 4-mL glass vial and dissolved in C₆D₆ (0.5 mL). The diaryl(chloro)borane (30 μmol, 1 equiv) is added at room temperature to the orange C₆D₆ solution of **1**^R in one portion. The solution is then stirred vigorously for 5 min, time during which color change (from orange to either red or green) and gas evolution (N₂) are observed. The mixture is then transferred to an NMR tube equipped with a J. Young valve and analyzed by NMR spectroscopy to check for the complete formation of the *trans*-chloro boryldiazenido complex **2**^{Et}, **3**^{Ph} or **3**^{Et}. Back to the glove box, the mixture is transferred from the NMR tube to a 4-mL glass vial. The NMR tube is rinsed with a minimal amount of toluene that is next added to the reaction solution in the vial. The latter is layered with pentane (3 mL) and the resulting mixture is kept at -40 °C over few days, affording crystals of **2**^{Et}, **3**^{Ph} or **3**^{Et}. After removal of the supernatant, part of the crystalline material is submitted to an X-ray diffraction analysis. The rest is washed with pentane (2 × 1 mL) and dried under vacuum, affording **2**^{Ph}, **2**^{Et}, **3**^{Ph} or **3**^{Et} as a pure compound.

II.3. Characterization of the complexes [W(Cl){N₂B(Ar)₂}{R₂P(CH₂)₂PR₂}] ({Ar,R} = {Mes,Et}, 2^{Et}; {Ar,R} = {C₆F₅,Ph}, 3^{Ph}; {Ar,R} = {C₆F₅,Et}, 3^{Et}).

II.3.1 [W(Cl){N₂BMes₂}(depe)₂] (**2**^{Et})

Yellow crystals, isolated yield 68% (18 mg, 20 μmol). ¹H NMR (400 MHz, C₆D₆) δ = 6.78 (s, *m*-Ar, 4H), 2.45 (s, 12H, *o*-Ar-CH₃), 2.23 (s, 6H, *p*-Ar-CH₃), 2.18 – 2.04 (m, 8H, CH₃-CH₂-), 1.84 – 1.64 (m, 8H, CH₃-CH₂-), 1.47 (t, *J* = 7.3 Hz, 8H, P-CH₂-CH₂-P), 1.04 – 0.93 (m, 24H, CH₃-CH₂-). ¹¹B NMR (128 MHz, C₆D₆) no signal could be detected. ³¹P{¹H} NMR (162 MHz, C₆D₆) δ 35.6 (¹J_{WP} = 143.2 Hz). ¹³C NMR (101 MHz, C₆D₆) δ = 145.0 (*ipso*-Ar^{Mes}), 140.5 (*o*-Ar^{Mes}), 135.3 (*p*-Ar^{Mes}), 127.9 (*m*-Ar^{Mes}), 24.6 (q, ¹J_{CP} = 9.3 Hz, P-CH₂-CH₂-P), 23.9 (*o*-Ar-CH₃), 21.3 (*p*-Ar-CH₃), 18.6 (dq, ¹J_{CP} = 47.0, ³J_{CP} = 5.9 Hz, CH₃-CH₂-), 9.1 (d, ²J_{CP} = 50.7 Hz, CH₃-CH₂-). IR (ATR) ν/cm⁻¹ = 2933, 2900, 2875, 1604, 1449, 1413, 1241, 1197, 1141, 1027, 831, 807, 728, 663. Elem. Anal. Calcd. for C₃₈H₇₀BClN₂P₄W: C, 50.21; H, 7.76; N, 3.08; Found: C, 50.48; H, 6.96; N, 3.09.

II.3.2 [W(Cl){N₂B(C₆F₅)₂}(dppe)₂] (**3**^{Ph})

Yellow crystals, isolated yield 71% (29 mg, 21 μmol). ¹H NMR (400 MHz, C₆D₆) δ = 7.41 – 7.33 (m, 8H, Ar), 7.25 – 7.18 (m, 8H, Ar), 6.96 – 6.89 (m, 12H, Ar), 6.82 (t, *J*_{HH} = 7.5 Hz, 12H, Ar), 2.58 – 1.36 (m, 8H P-CH₂-CH₂-P). ¹¹B NMR (128 MHz, C₆D₆) no signal could be detected. ¹⁹F NMR (377 MHz, C₆D₆) δ = -132.4 (dd, *J*_{FF} = 26.4, *J*_{FF} = 9.0 Hz, 4F_{ortho}), -156.7 (t, *J*_{FF} = 20.9 Hz, 2F_{para}), -163.2 - -163.5 (m, 4F_{meta}). ³¹P{¹H} NMR (162 MHz, C₆D₆) δ = 34.6 (*J*_{WP} = 285 Hz). IR (ATR) ν/cm⁻¹ = 3051, 1642, 1510, 1465, 1432, 1381, 1296, 1082, 965, 805, 738, 693. Elem. Anal. Calcd. for C₆₄H₄₈BClF₁₀N₂P₄W: C, 55.34; H, 3.48; N, 2.02; Found: C, 55.44; H, 3.07; N, 2.02.

II.3.1 [W(Cl){N₂B(C₆F₅)₂}(depe)₂] (**3**^{Et})

Green crystals, isolated yield 81% (24 mg, 24 μmol). **^1H NMR** (400 MHz, C_6D_6) δ = 1.95–1.70 (m, 16H, $\text{CH}_3\text{-CH}_2\text{-}$), 1.43–1.22 (m, 8H, $\text{P-CH}_2\text{-CH}_2\text{-P}$), 1.03 (m, $^3J_{\text{HH}} = ^3J_{\text{HP}} = 9.8$ Hz, 12H, $\text{CH}_3\text{-CH}_2\text{-}$), 0.91 (m, $^3J_{\text{HH}} = ^3J_{\text{HP}} = 9.8$ Hz, 12H, $\text{CH}_3\text{-CH}_2\text{-}$). **^{11}B NMR** (128 MHz, C_6D_6) δ = 21.8. **^{19}F NMR** (377 MHz, C_6D_6) δ = –133.4 (dd, $J_{\text{FF}} = 25.9$, $J_{\text{FF}} = 9.8$ Hz, $4F_{\text{ortho}}$), –157.1 (t, $J_{\text{FF}} = 20.4$ Hz, $2F_{\text{para}}$), –163.7 (ddd, $J_{\text{FF}} = 26.2$, 20.3, 9.4 Hz, $4F_{\text{meta}}$). **$^{31}\text{P}\{^1\text{H}\}$ NMR** (162 MHz, C_6D_6) δ = 33.3 ($J_{\text{PW}} = 282.5$ Hz). **IR** (ATR) ν/cm^{-1} = 2961, 2938, 2904, 2881, 1642, 1511, 1463, 1378, 1290, 1117, 1080, 1030, 965, 846, 736, 695. **Elem. Anal.** Calcd. for $\text{C}_{32}\text{H}_{48}\text{BClF}_{10}\text{N}_2\text{P}_4\text{W}$: C, 38.25; H, 4.82; N, 2.79; Found: C, 38.64; H, 4.85; N, 2.73.

II.4. General procedure for the reaction of compounds **2^{Et}**, **3^{Ph}** and **3^{Et}** with **TIBAr^F₄**

Caution: Thallium compounds are notoriously highly toxic, even by skin contact. Proper protective and disposal measures have to be taken by the experimenter.

In a glove box, the *trans*-chloro boryldiazenido complex (56 μmol) is weighed in a 4-mL glass vial and dissolved in C_6D_6 or $\text{C}_6\text{D}_5\text{Cl}$ (0.5 mL). **TIBAr^F₄** (56 μmol , 1.0 equiv) is added at room temperature to the solution in one portion. The resulting mixture is then stirred vigorously for 5 min, then transferred to an NMR tube equipped with a J. Young valve and analyzed by NMR spectroscopy to check for the complete conversion of the starting complex. The reaction of **3^{Et}** with **TIBAr^F₄** did not show signs of adduct formation according to NMR analysis. The mixture is transferred in the glove box from the NMR tube to a 4-mL glass vial. The NMR tube was rinsed with a minimal amount of toluene. Then pentane (2 mL) was added and the resulting mixture was kept at –40 °C over few days, affording crystals of the thallium adduct. After removal of the supernatant, part of the crystals are submitted to an X-ray diffraction analysis, while the rest is washed with pentane (2 \times 1 mL) and dried under vacuum, to give **[2^{Et}·TI]BAR^F₄** or **[3^{Ph}·TI]BAR^F₄** as a pure compound.

II.5. Characterization of the complexes **[TI(W{Cl}{N₂B(R)₂}{L₂})]BAR^F₄** (**{R,L} = {Mes,depe}** or **{C₆F₅,dppe}**) (**[2^{Et}·TI]BAR^F₄** and **[3^{Ph}·TI]BAR^F₄**).

II.5.1 **[W(Cl)(NN(TI){B(Mes)₂})(depe)₂]BAR^F₄** (**[2^{Et}·TI]BAR^F₄**)

Orange crystals, isolated yield 53% (33 mg, 29 μmol). **^1H NMR** (400 MHz, $\text{C}_6\text{D}_5\text{Cl}$) δ = 8.31–8.19 (m, 8H, *o*-Ar^F), 7.62 (s, 4H, *p*-Ar^F), 6.69 (s, 4H, *m*-Ar^{Mes}), 2.14 (s, 6H, *o*-CH₃), 2.06 (s, 12H, *p*-CH₃), 1.95 (m, 5H, $\text{CH}_3\text{-CH}_2\text{-}$), 1.76 (m, 5H, $\text{CH}_3\text{-CH}_2\text{-}$), 1.70–1.48 (m, 12H, $\text{P-CH}_2\text{-CH}_2\text{-P} + \text{CH}_3\text{-CH}_2\text{-P}$), 1.38 (m, 5H, $\text{CH}_3\text{-CH}_2\text{-P}$), 0.94 (d, $J = 5.9$ Hz, 24H, $\text{CH}_3\text{-CH}_2\text{-}$). **^{11}B NMR** (128 MHz, $\text{C}_6\text{D}_5\text{Cl}$) δ = –5.90 (BAR^F₄). **^{13}C NMR** (101 MHz, $\text{C}_6\text{D}_5\text{Cl}$) δ = 167.4 (q, $J_{\text{CB}} = 49.8$ Hz, *ipso*-Ar^F), 147.0 (s, *ipso*-Ar^{Mes}), 144.4 (s, *m*-Ar^{Mes}), 143.7 (s, *o*-Ar^{Mes}), 140.2 (s, *o*-Ar^F), 134.7 (s, *m*-Ar^{Mes}), 131.3 (s, C_{IV} -Ar^F), 128.5 (s, *o*-Ar^F), 122.7 (s, $J_{\text{CF}} = 3.8$ Hz, *p*-Ar^F), 27.9 (s, *o*-CH₃), 25.9 (s, *p*-CH₃), 23.5 (t, $J_{\text{CP}} = 12.8$ Hz, $\text{P-CH}_2\text{-CH}_2\text{-P}$). **IR** (ATR) ν/cm^{-1} = 2974, 1608, 1352, 1274, 1115, 885, 837, 743, 713, 682. **^{19}F NMR** (377 MHz, $\text{C}_6\text{D}_5\text{Cl}$) δ = –61.9 (s, CF₃). **$^{31}\text{P}\{^1\text{H}\}$ NMR** (162 MHz, $\text{C}_6\text{D}_5\text{Cl}$) δ = 31.3 ($J_{\text{PW}} = 137.4$ Hz). **Elem. Anal.** Calcd. for $\text{C}_{70}\text{H}_{82}\text{B}_2\text{ClF}_{24}\text{N}_2\text{P}_4\text{TIW}$: C, 42.54; H, 4.18; N, 1.42; Found: C, 42.36; H, 3.95; N, 0.95.

II.5.2 **[W(CITl){N₂B(C₆F₅)₂}(dppe)₂]BAR^F₄** (**[3^{Ph}·TI]BAR^F₄**)

Yellow crystals, isolated yield 50% (44 mg, 28 μmol). **^1H NMR** (400 MHz, C_6D_6) δ = 8.40 (m, 8H, *o*-Ar^F), 7.68 (s, 4H, *p*-Ar^F), 7.35 (m, 8H, *m*-Ar), 6.99–6.97 (m, 4H, *p*-Ar), 6.95 (s, 8H, *o*-Ar), 6.91–6.87 (m, 4H, *p*-Ar), 6.85 (m, 8H, *m*-Ar), 6.79 (m, 8H, *o*-Ar), 2.59–2.41 (m, 8H, $\text{P-CH}_2\text{-CH}_2\text{-P}$). **^{11}B NMR** (128 MHz,

C_6D_6) δ 23.5, - 5.9. **^{13}C NMR** (101 MHz, C_6D_6) δ = 162.8 (q, J_{CB} = 49.5 Hz, *ipso*-Ar^F), 135.5 (s, *o*-Ar^F), 133.8 (dt, J_{CP} = 21.9, 2.2 Hz, *m*-Ph), 130.3 (s, *o*-Ph), 129.6 (s, *p*-Ph), 128.6 (s, *p*-Ph), 127.9 (s, *o*-Ph), 126.6 (C_{IV} -Ar^F), 123.9 (C_{IV} -Ar^F), 118.0 (m, *p*-Ar^F), 31.6 (quint, J_{CP} = 9.7 Hz, P-CH₂-CH₂-P). **IR** (ATR) ν/cm^{-1} = 3056, 1643, 1513, 1469, 1434, 1353, 1275, 1120, 967, 885, 838, 807, 741. **^{19}F NMR** (377 MHz, C_6D_6) δ = -62.0 (s, CF₃), -132.4 (dd, J_{FF} = 26.0, 9.1 Hz, 4F_{*ortho*}), -155.7 (t, J_{FF} = 20.8 Hz, 2F_{*para*}), -162.8 - -163.1 (m, 4F_{*meta*}). **$^{31}P\{^1H\}$ NMR** (162 MHz, C_6D_6) δ 35.9 (J_{WP} = 145 Hz). **Elem. Anal.** Calcd. for $C_{96}H_{60}B_2ClF_{34}N_2P_4TIW \cdot 0.2 C_6D_6$: C, 47.20; H, 2.44; N, 1.13; Found: C, 47.75; H, 3.05; N, 0.97.

III. Spectroscopic Data of New Compounds

III.1. $[W(Cl)\{N_2BMe_2\}(dppe)_2]$ (2^{Ph}) in the reaction mixture.

Figure S1. 1H NMR (400 MHz, C_6D_6).

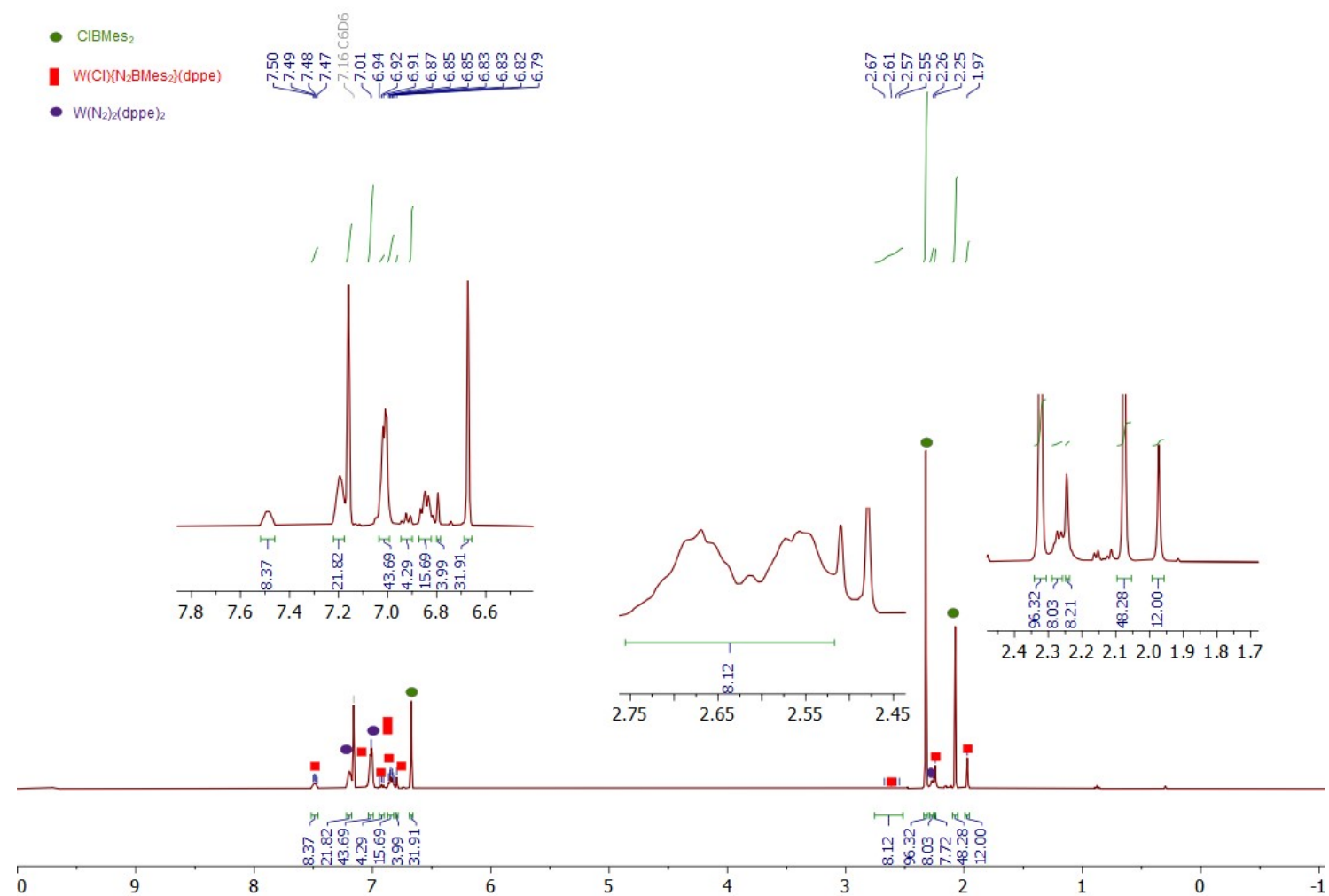


Figure S2. ^{11}B NMR (128 MHz, C_6D_6).

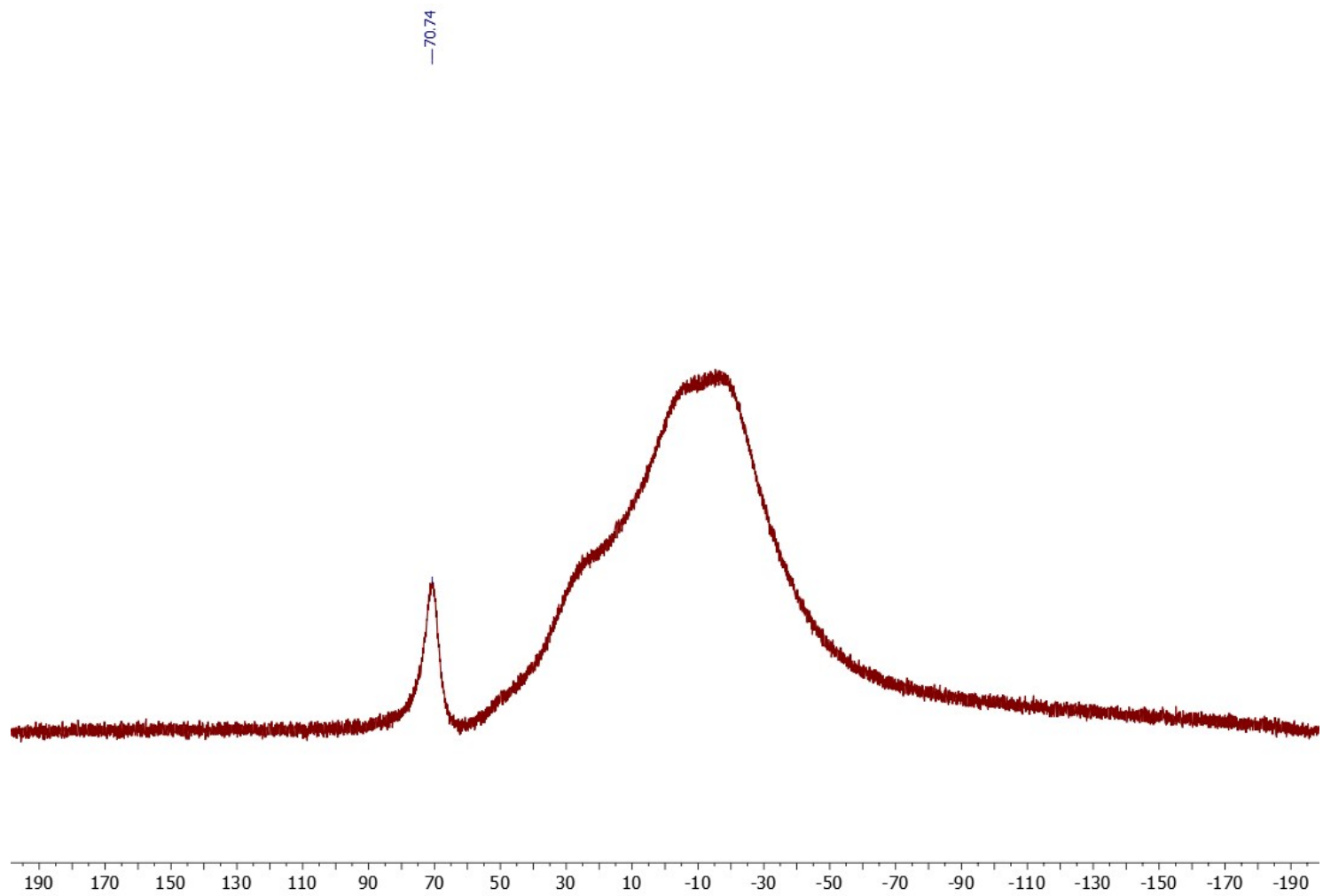


Figure S3. $^{13}\text{C}\{^1\text{H}\}$ NMR (100 MHz, C_6D_6).

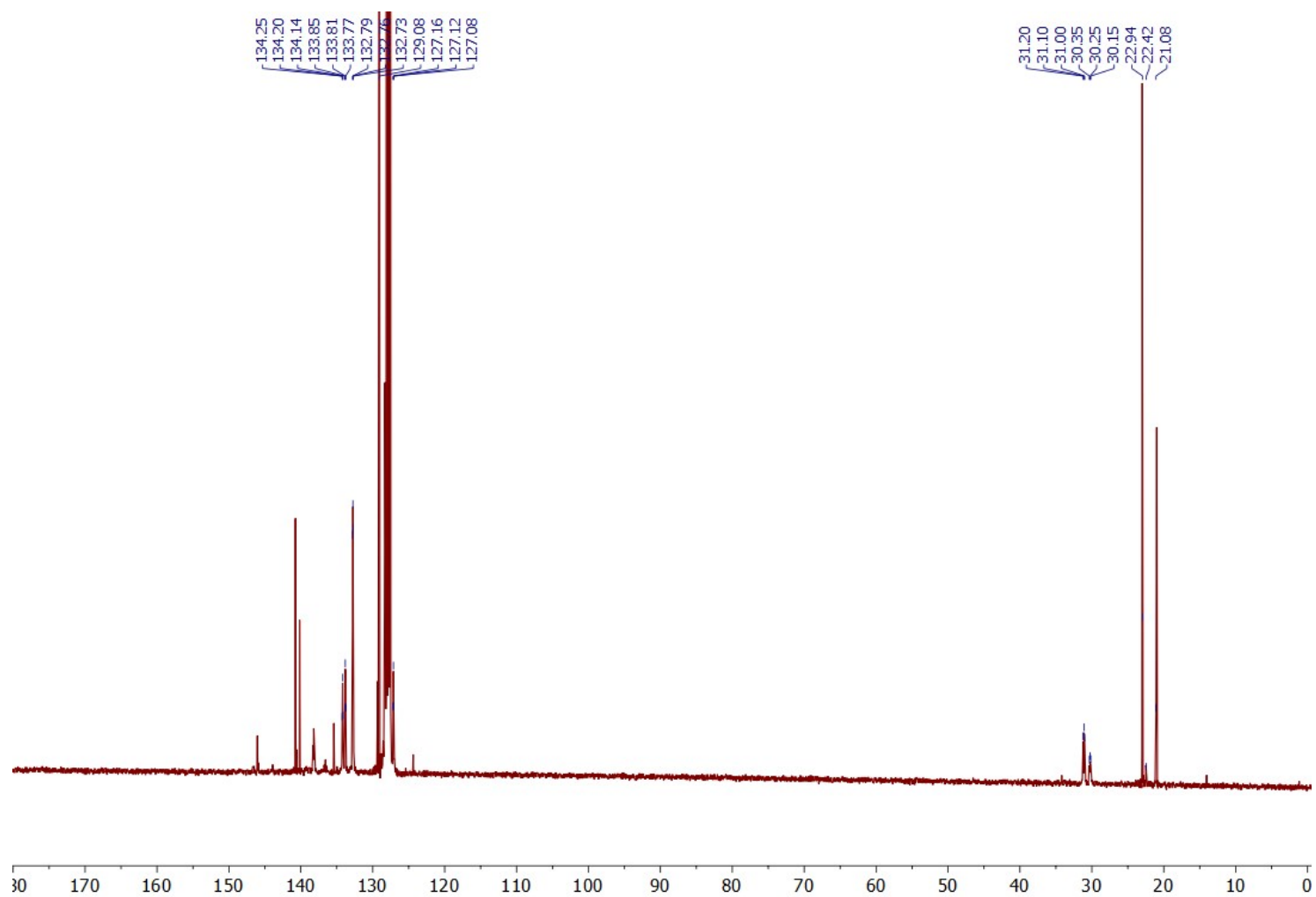


Figure S4. ^{31}P NMR (162 MHz, C_6D_6).

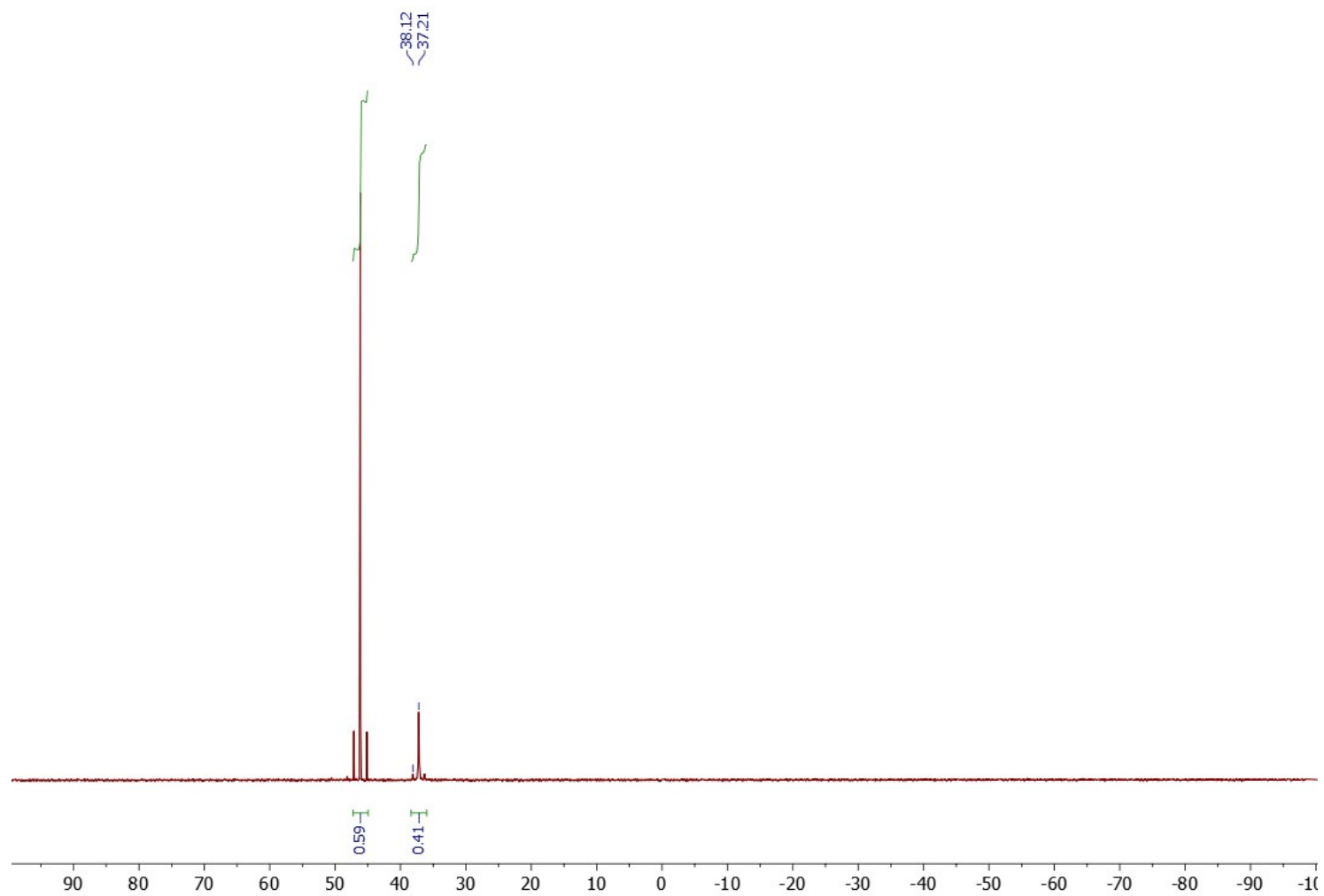
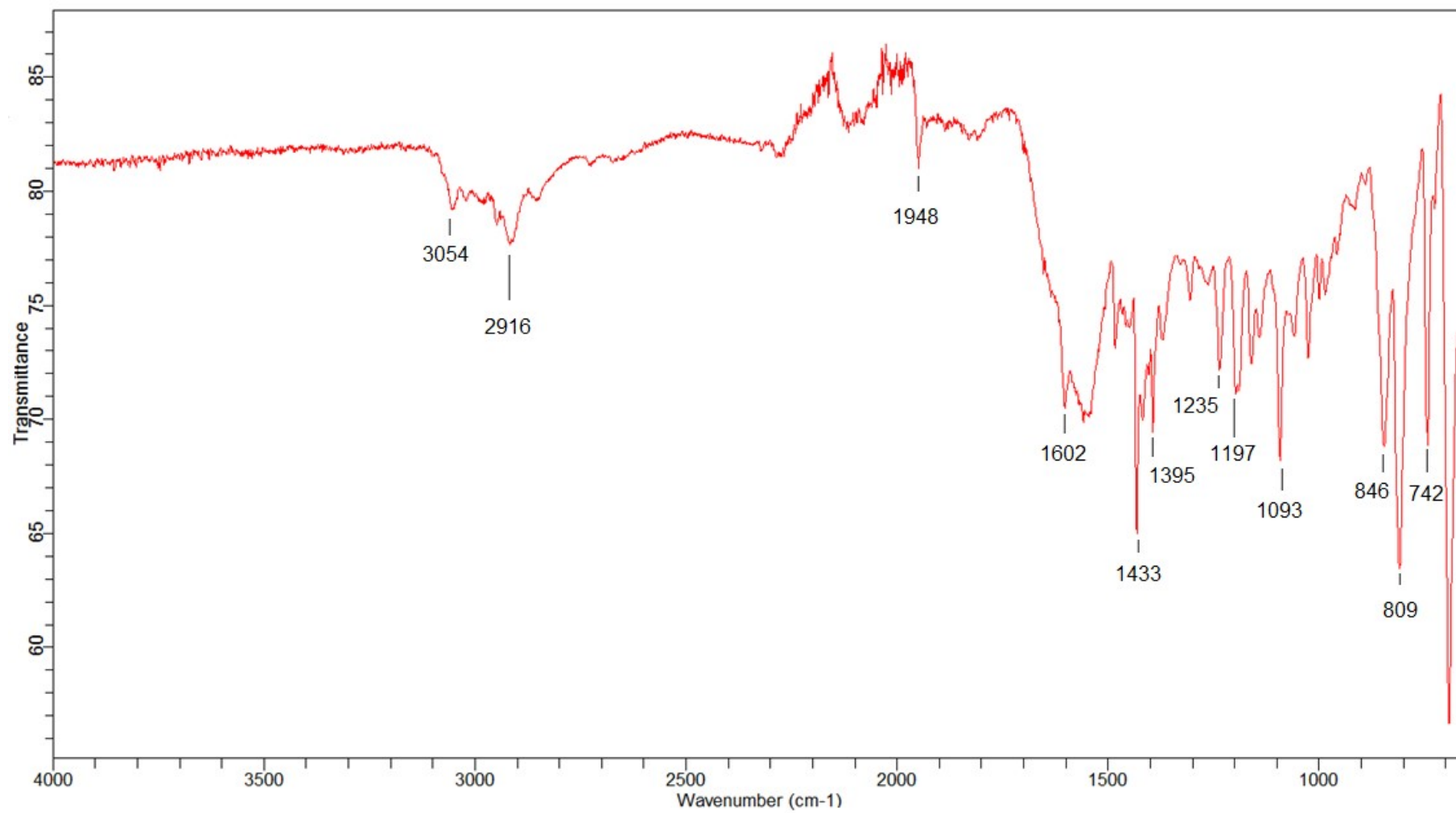


Figure S5. FT-IR (ATR, 400–4000 cm^{-1} range) of crystalline $[\text{W}(\text{Cl})\{\text{N}_2\text{BMes}_2\}(\text{dppe})_2]$ (2^{Ph}).



III.2. $[\text{W}(\text{Cl})\{\text{N}_2\text{BMes}_2\}(\text{depe})_2] (2^{\text{Et}})$

Figure S6. ^1H NMR (400 MHz, C_6D_6).

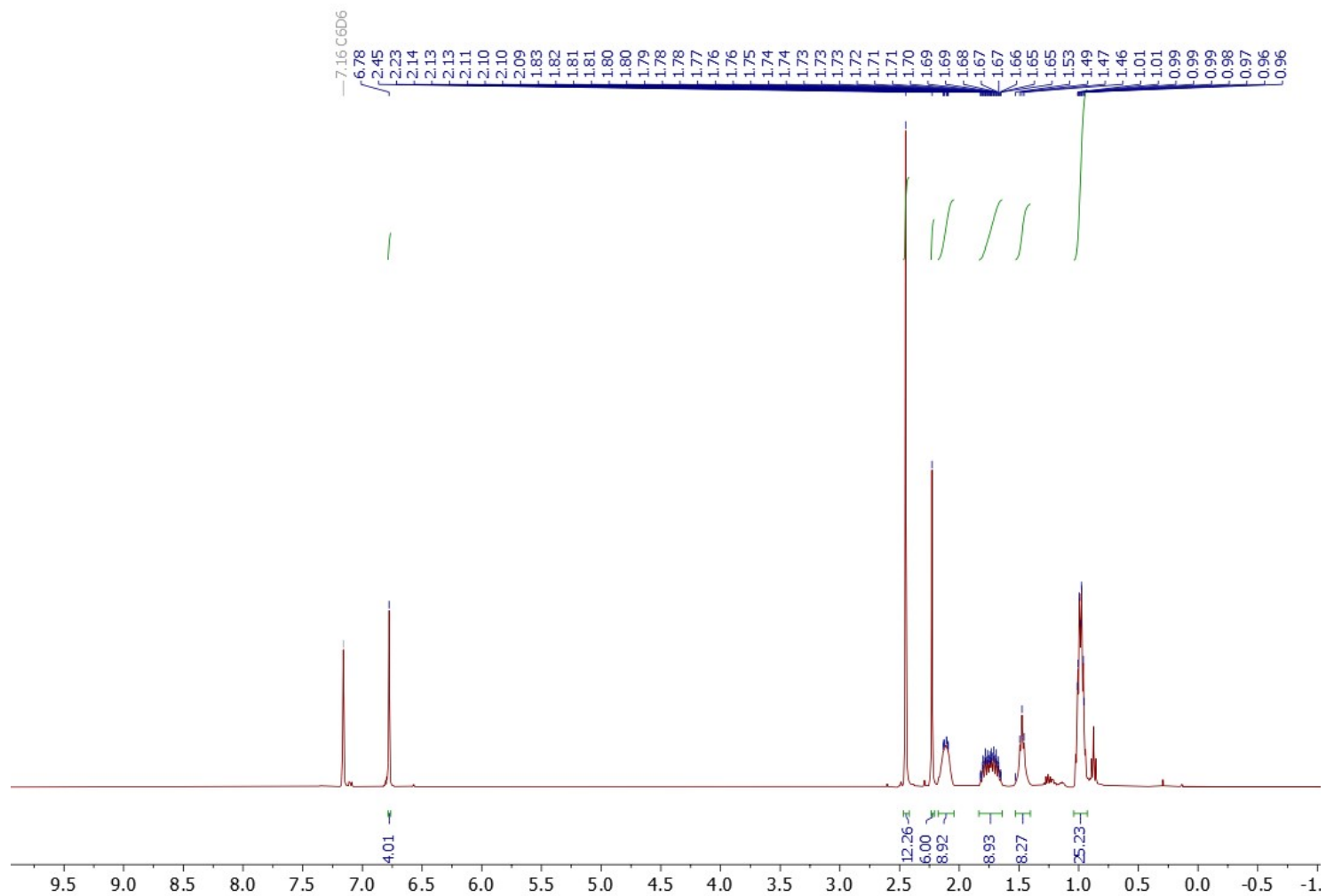


Figure S7. ^{11}B NMR (128 MHz, C_6D_6).

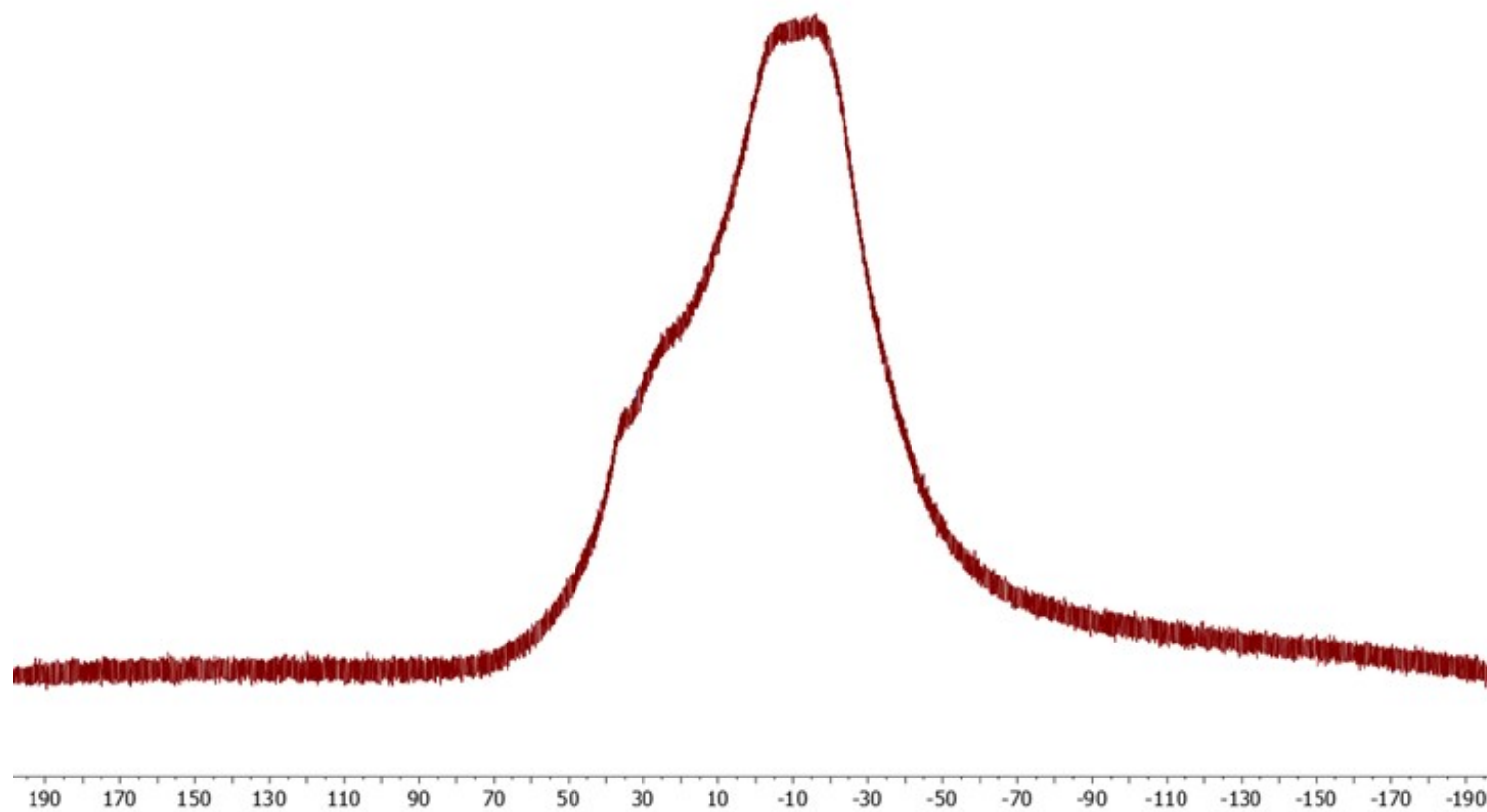


Figure S8. $^{13}\text{C}\{^1\text{H}\}$ NMR (100 MHz, C_6D_6).

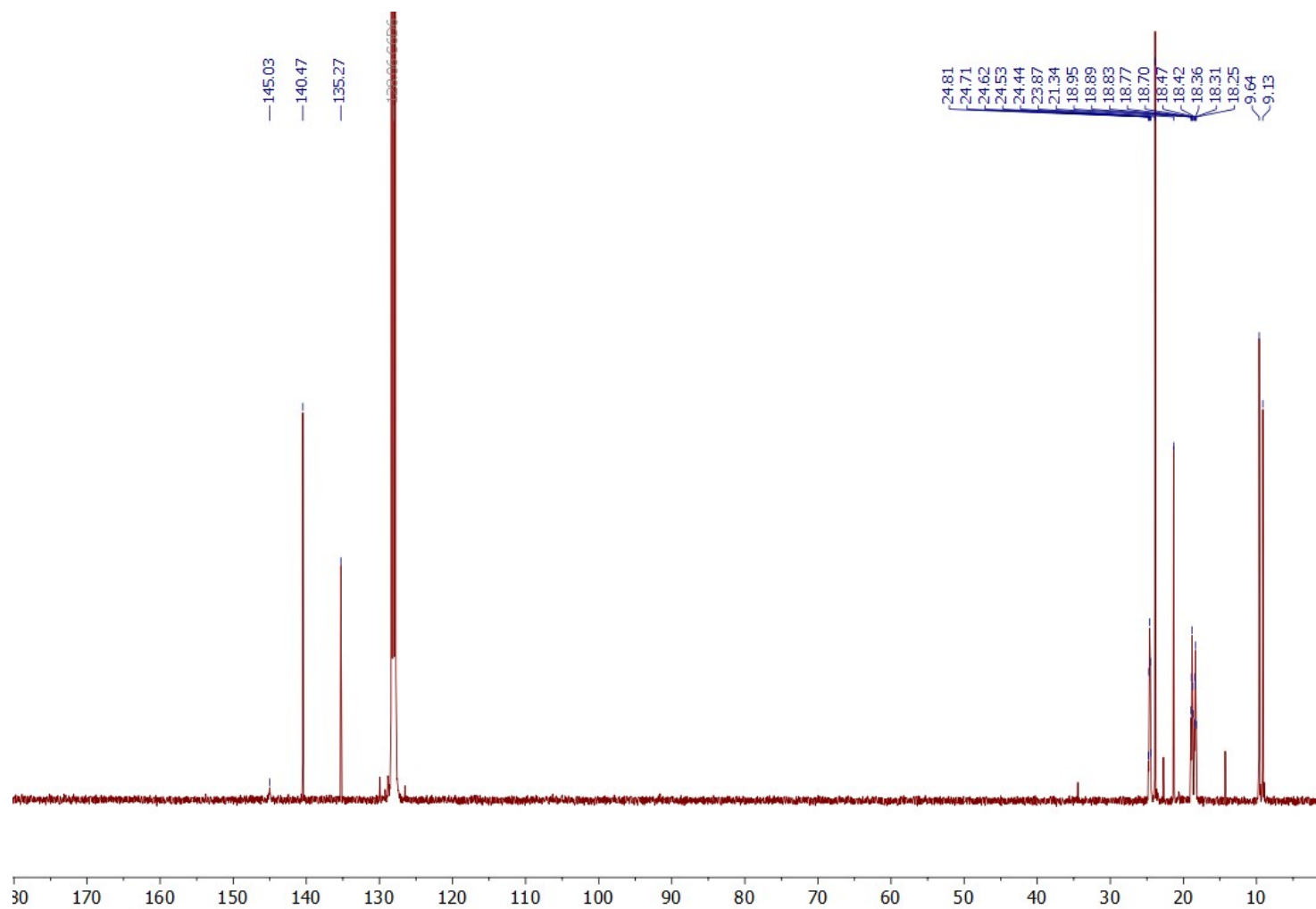


Figure S9. ^{31}P NMR (162 MHz, C_6D_6).

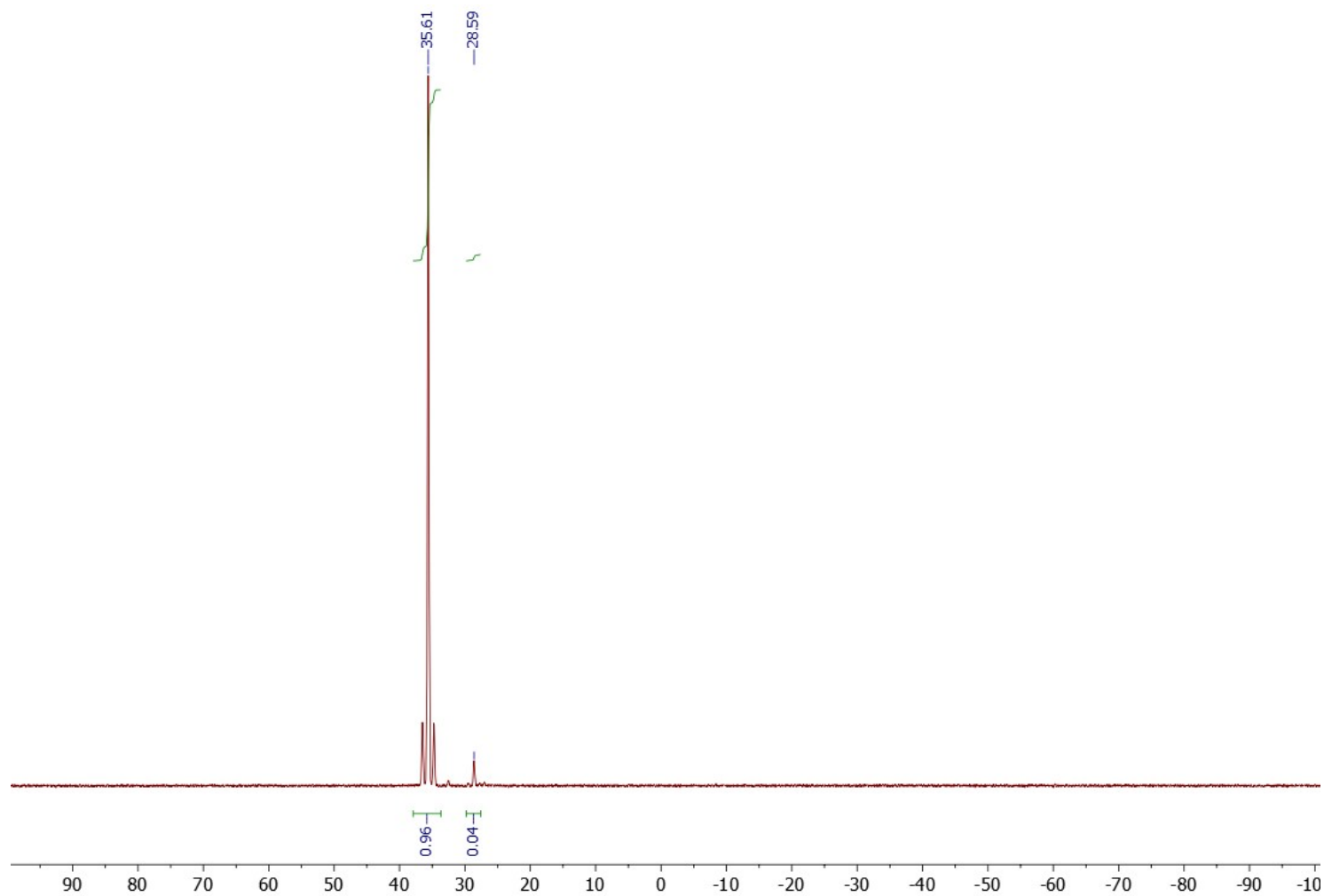
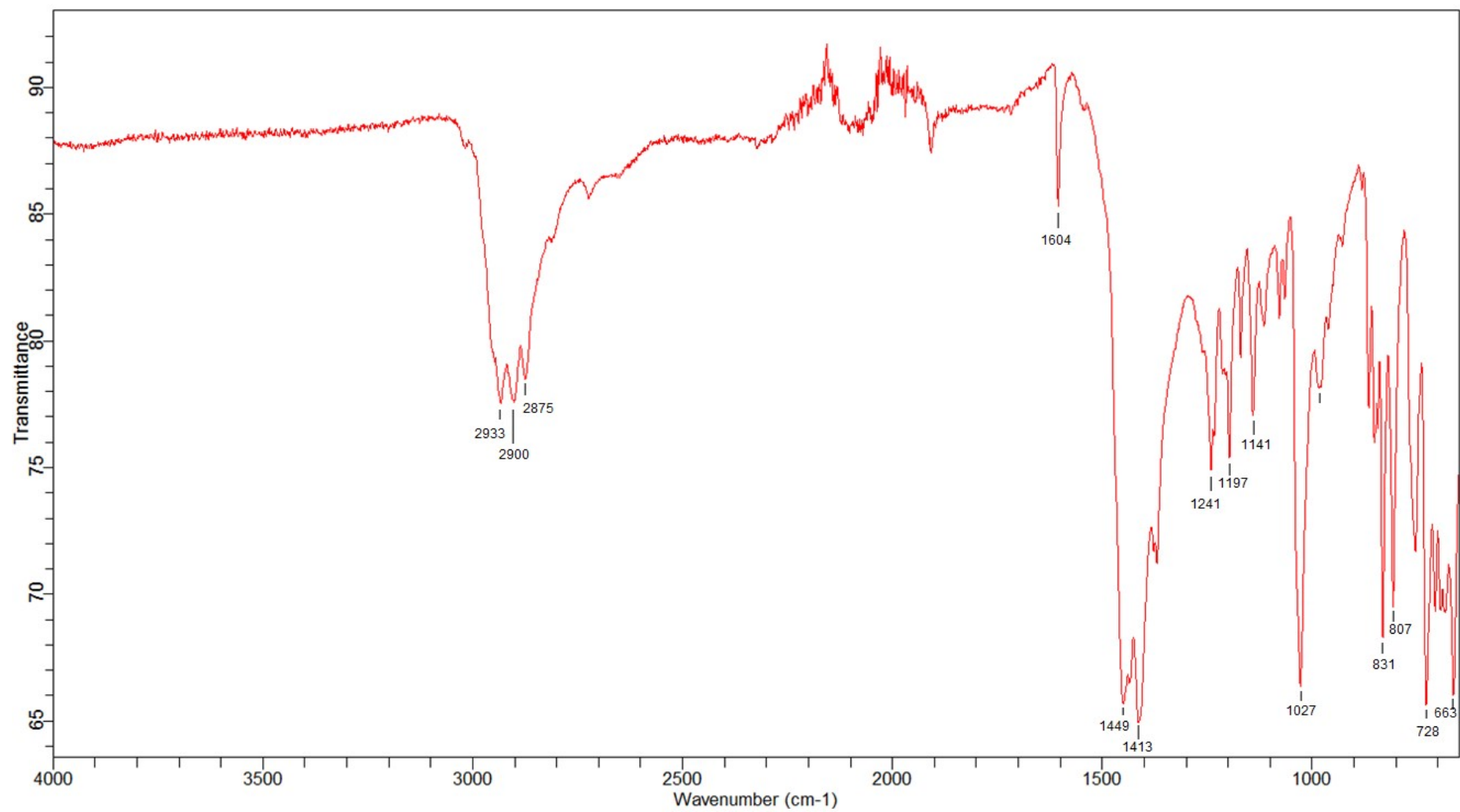


Figure S10. FT-IR (ATR, 400–4000 cm⁻¹ range).



III.3. $[\text{W}(\text{Cl})\{\text{N}_2\text{B}(\text{C}_6\text{F}_5)_2\}(\text{dppe})_2]$ (3^{Ph})

Figure S11. ^1H NMR (400 MHz, C_6D_6).

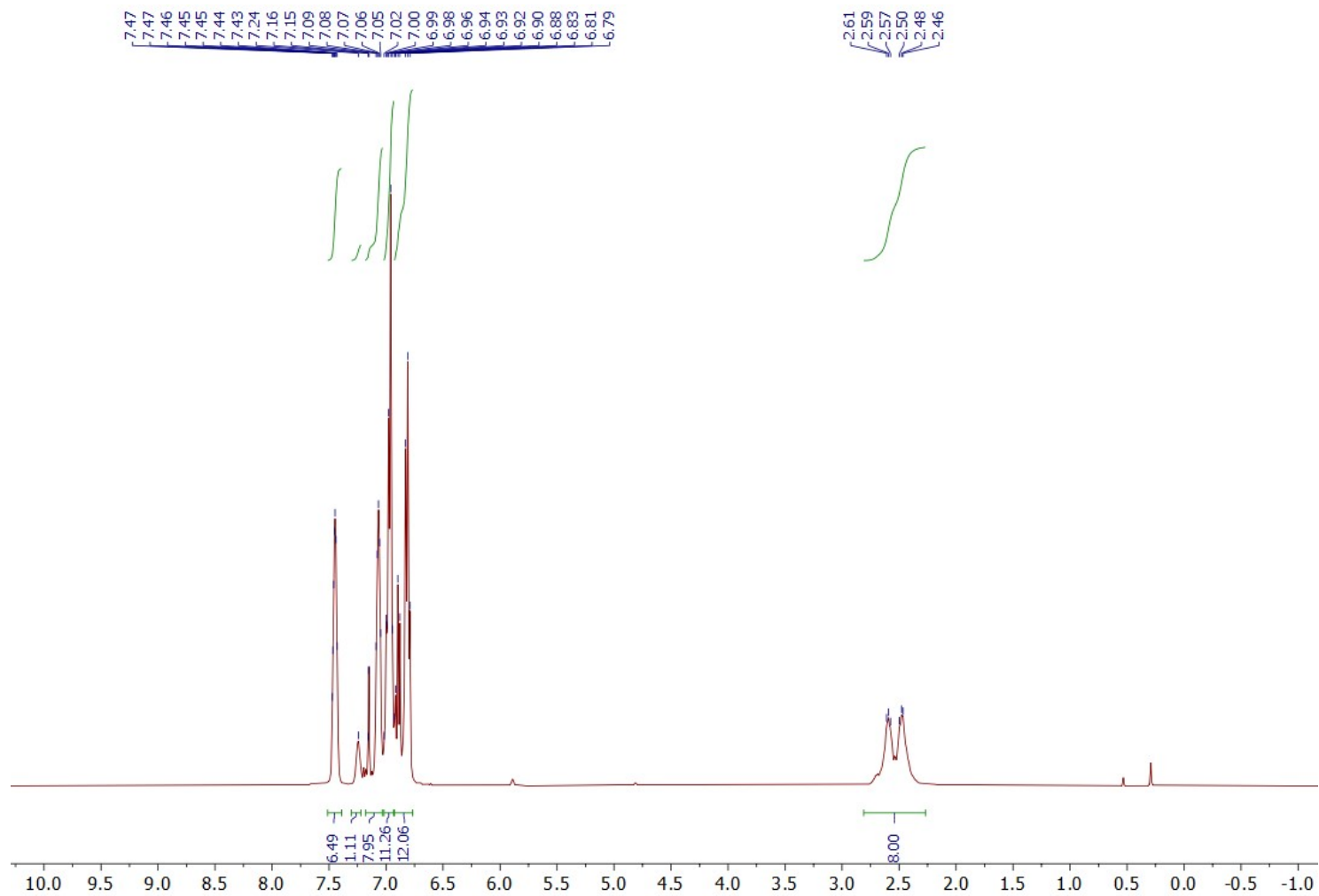


Figure S12. ^{11}B NMR (128 MHz, C_6D_6).

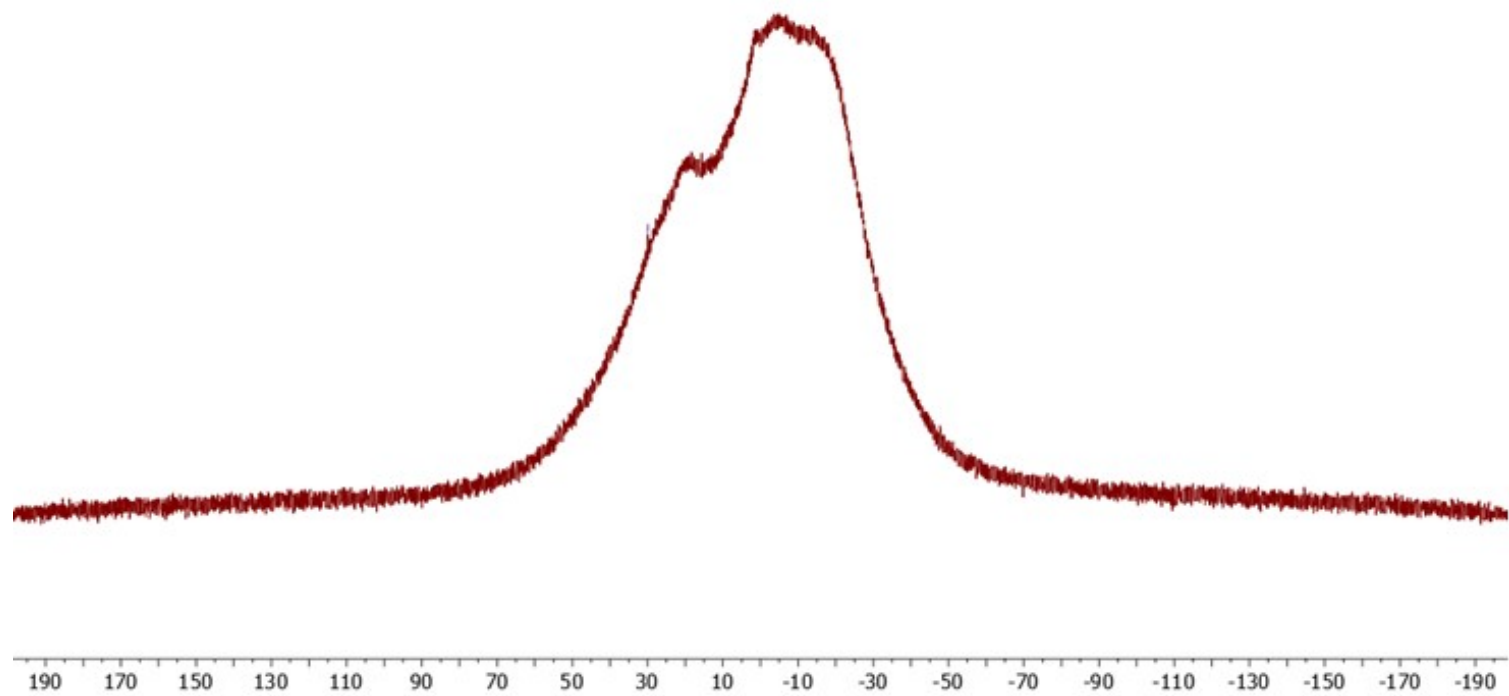


Figure S13. ^{19}F NMR (376 MHz, C_6D_6).

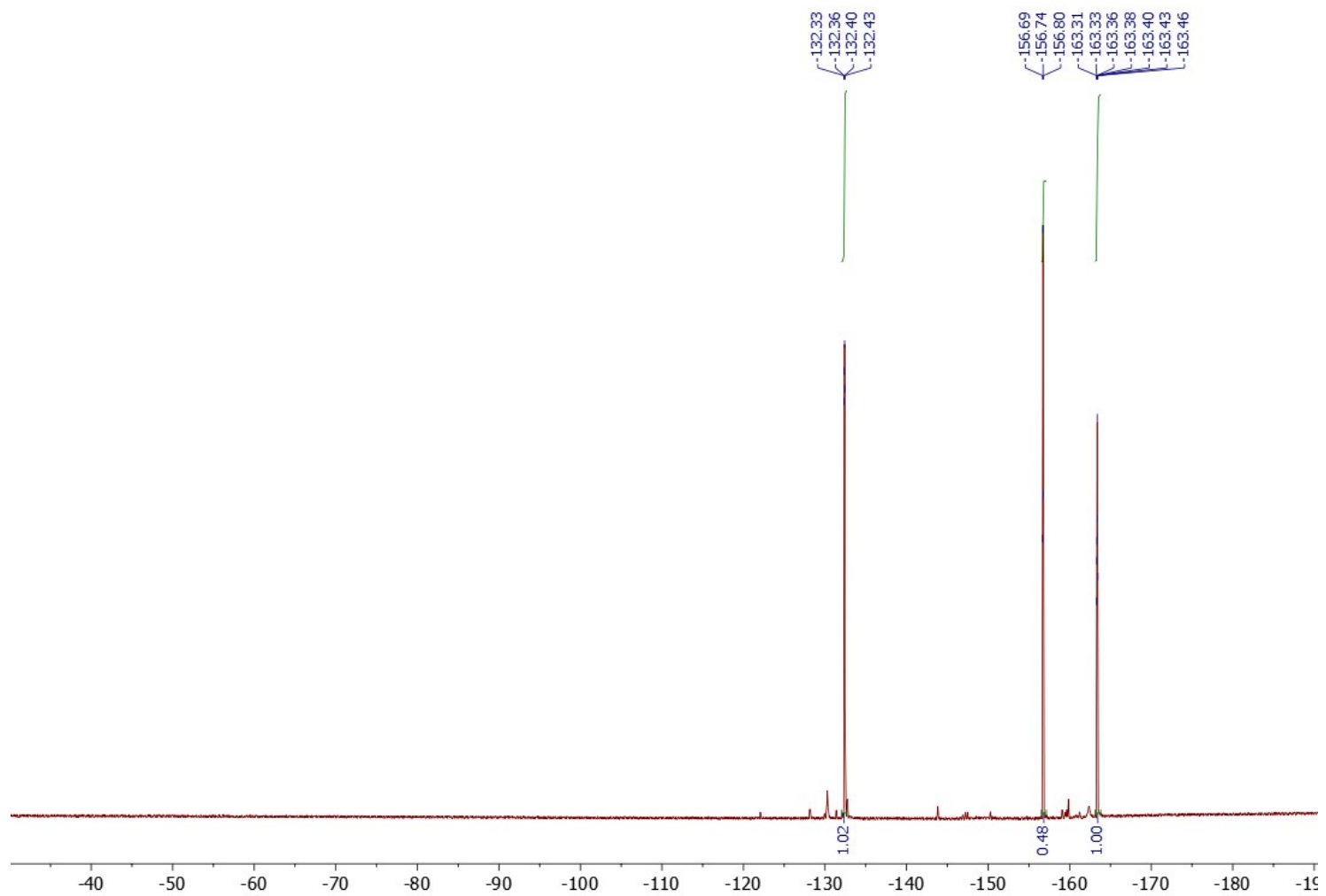


Figure S14. $^{31}\text{P}\{^1\text{H}\}$ NMR (162 MHz, C_6D_6)

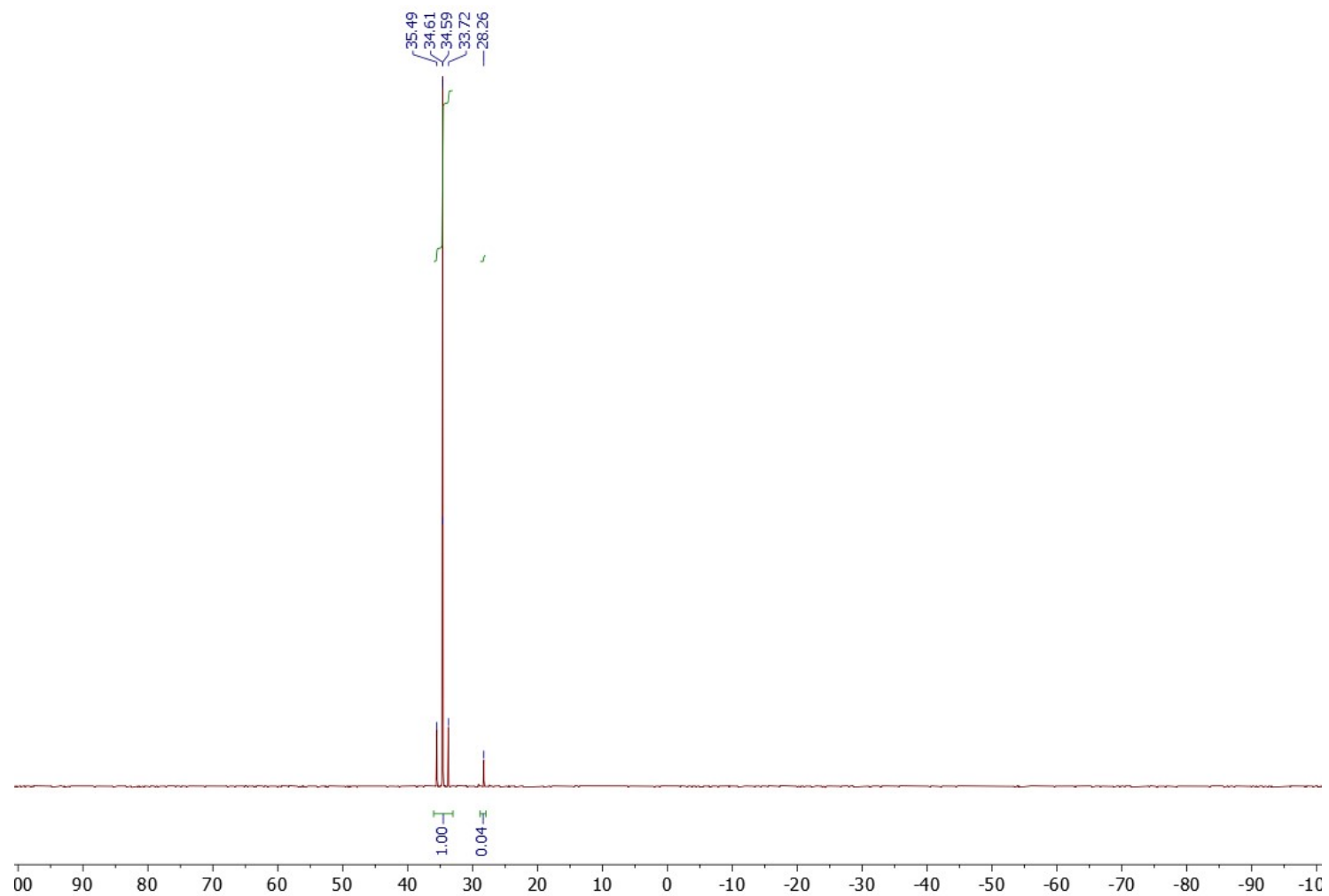
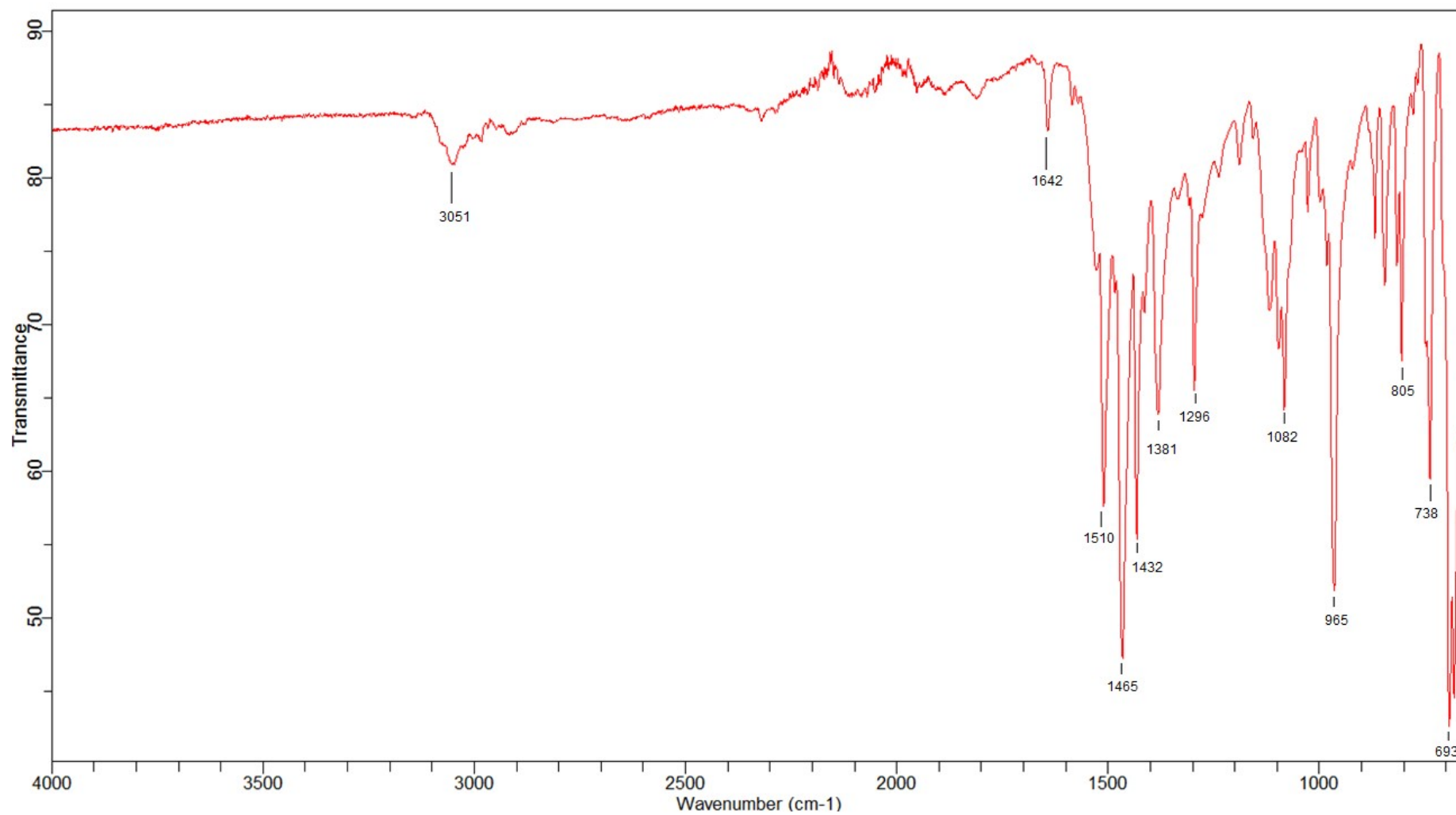


Figure S15. FT-IR (ATR, 400–4000 cm^{-1} range).



III.4. $[\text{W}(\text{Cl})\{\text{N}_2\text{B}(\text{C}_6\text{F}_5)_2\}(\text{depe})_2]$ (3^{Et})

Figure S16. ^1H NMR (400 MHz, C_6D_6).

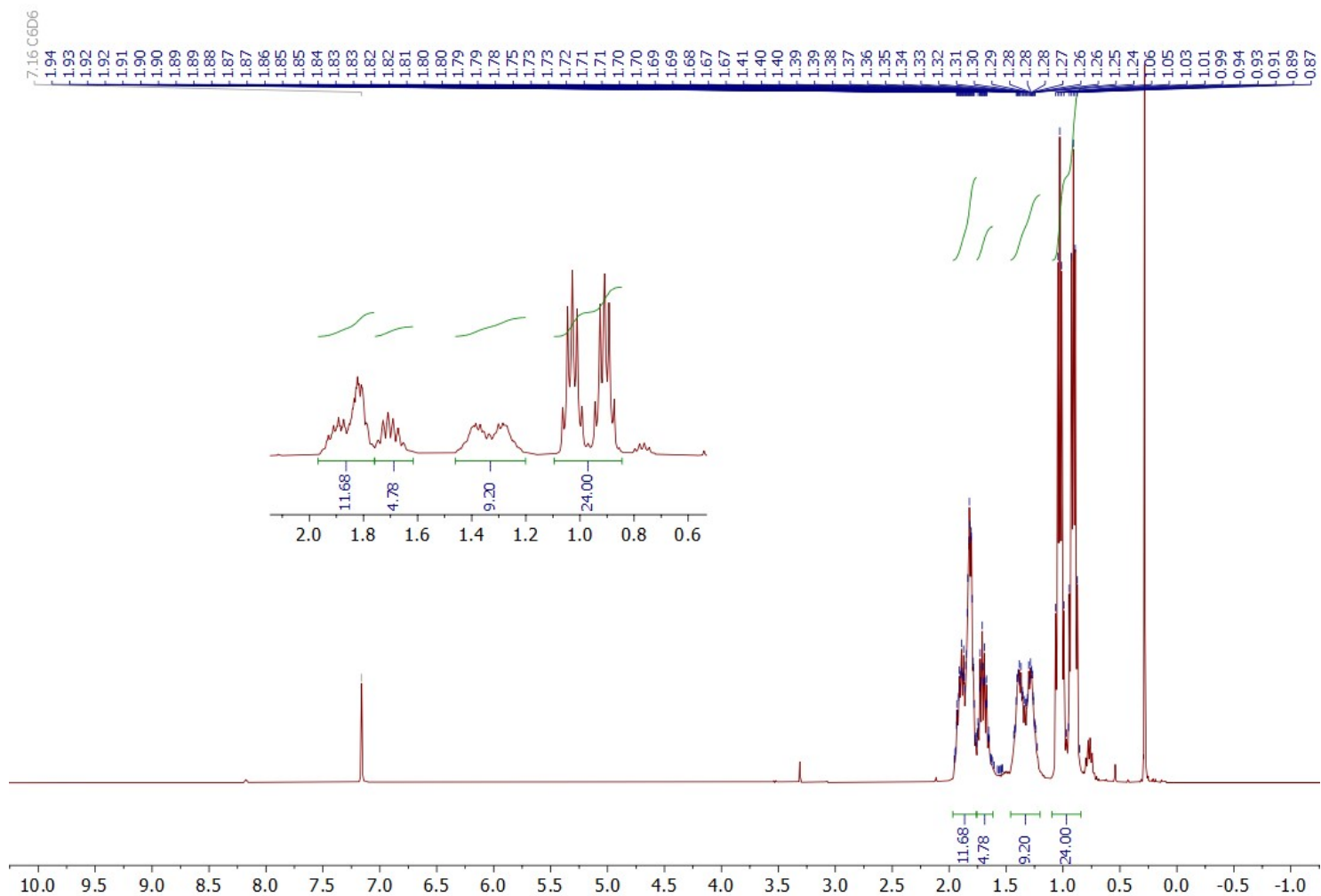


Figure S17. ^{11}B NMR (128 MHz, C_6D_6).

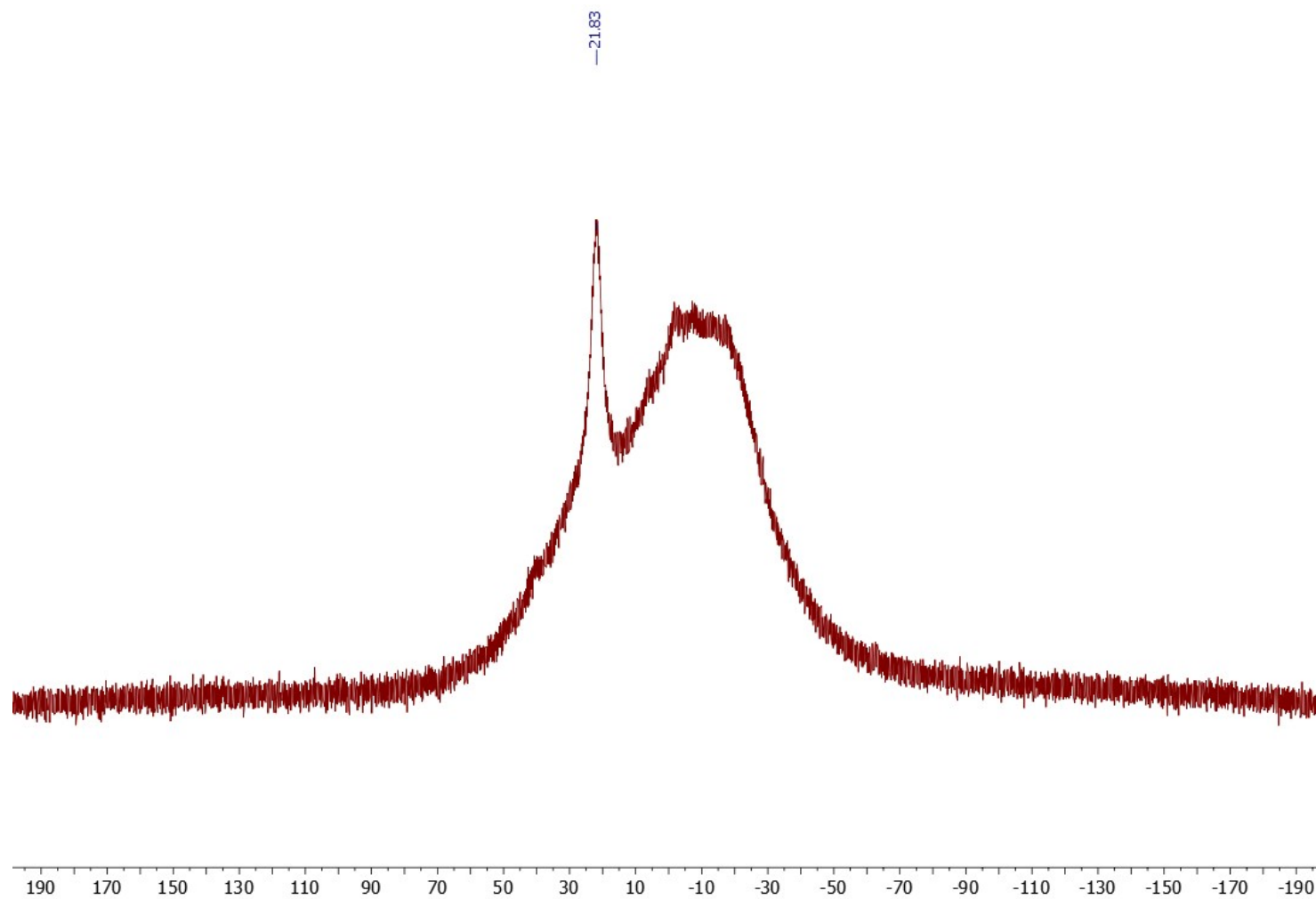


Figure S18. ^{19}F NMR (376 MHz, C_6D_6).

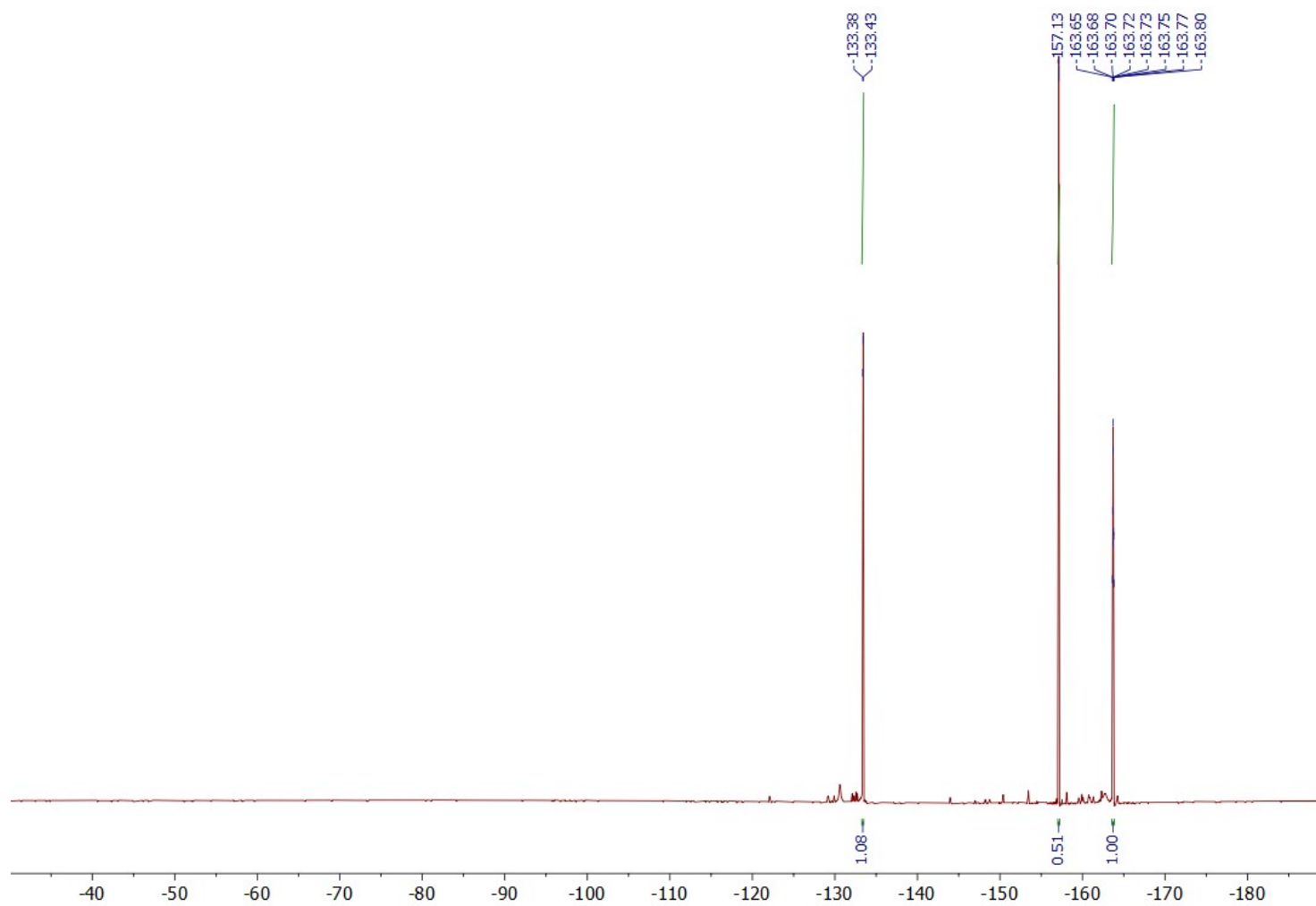


Figure S19. $^{31}\text{P}\{^1\text{H}\}$ NMR (162 MHz, C_6D_6).

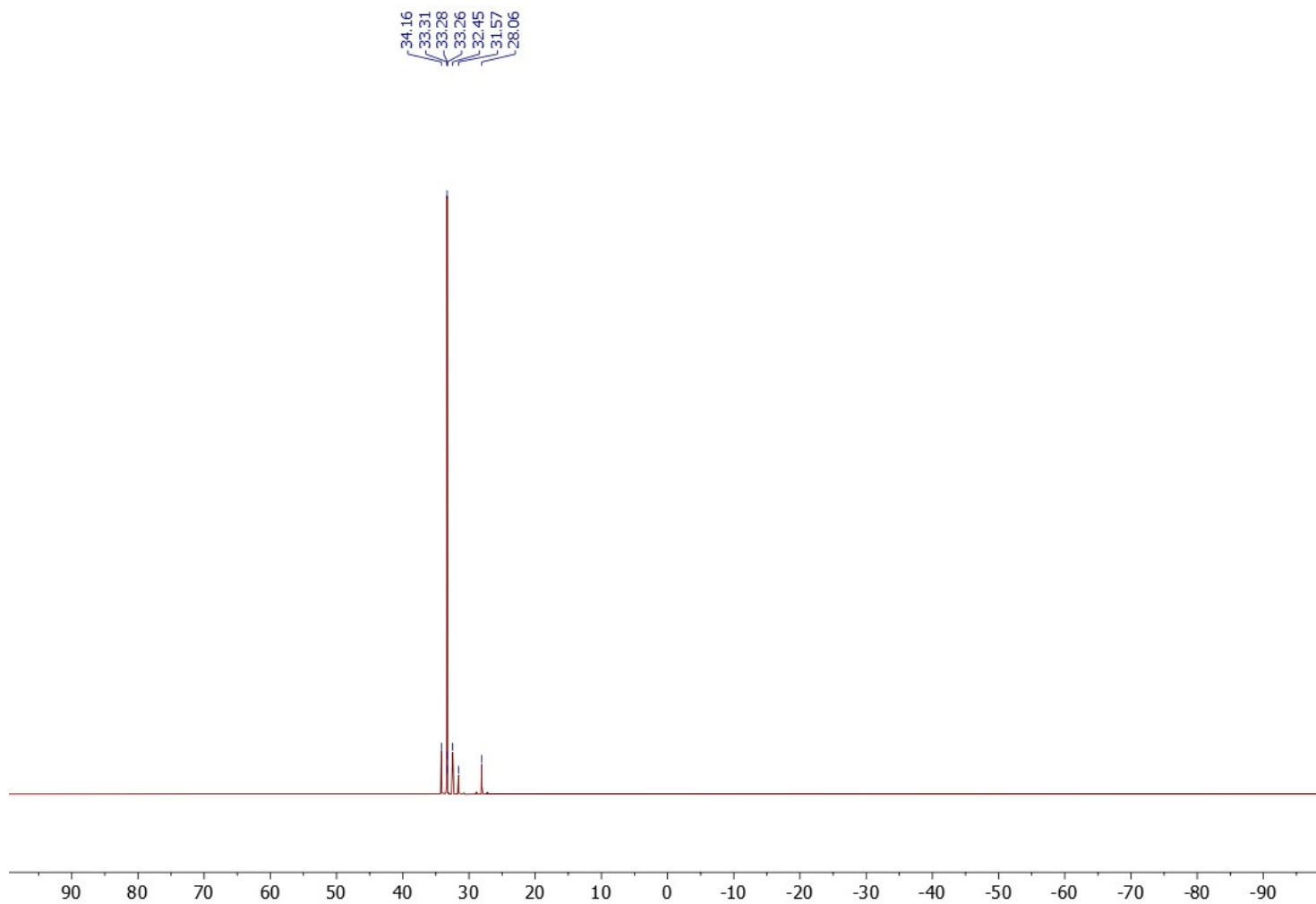
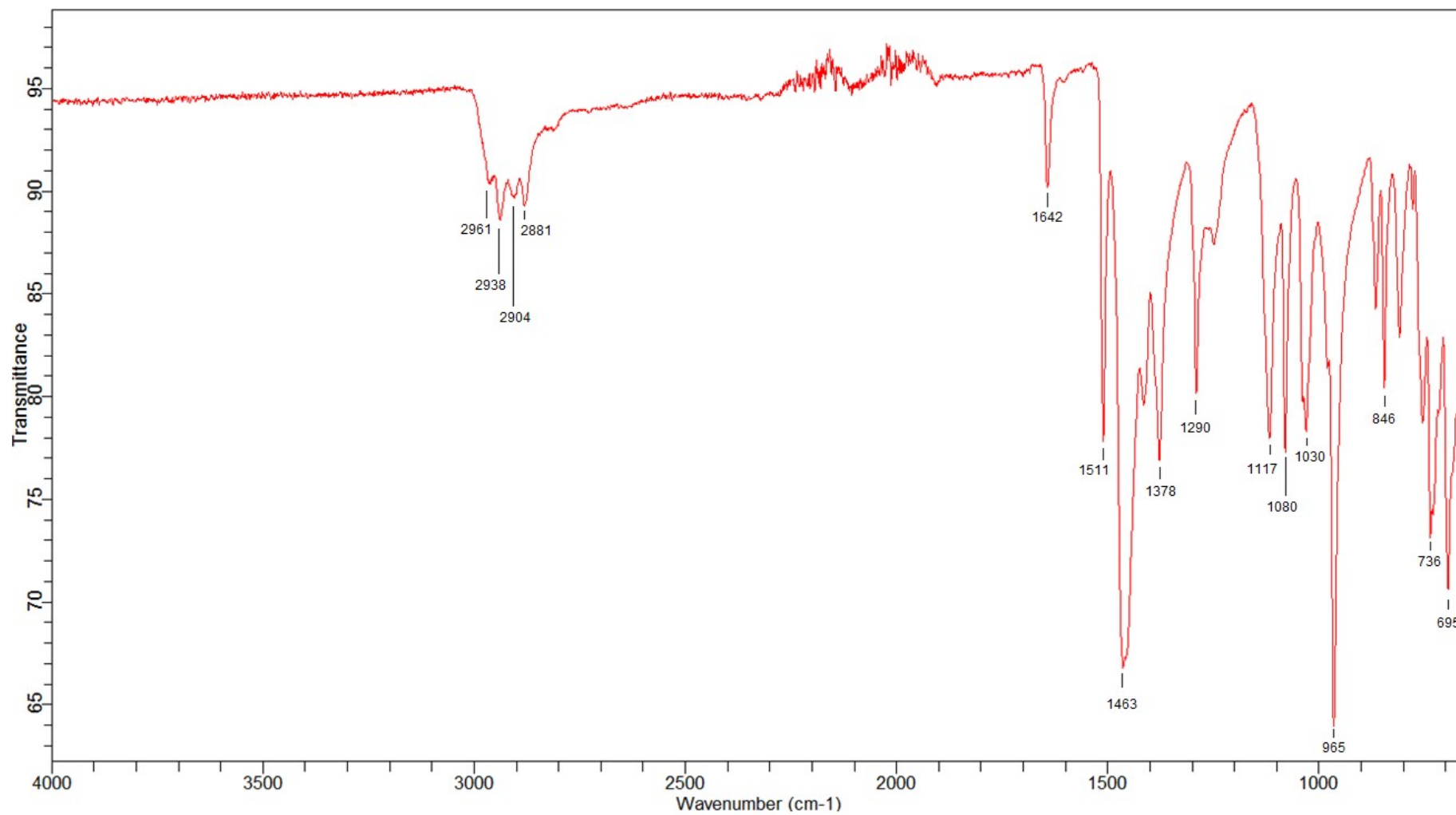


Figure S20. FT-IR (ATR, 400–4000 cm^{-1} range).



III.1. $[\text{W}(\text{Cl})(\text{NN}(\text{TI})\{\text{B}(\text{Mes})_2\})_2](\text{depe})_2$ ($[\text{2}^{\text{Et}}\text{-TI}]\text{BAr}^{\text{F}}_4$)

Figure S21. ^1H NMR (400 MHz, $\text{C}_6\text{D}_5\text{Cl}$).

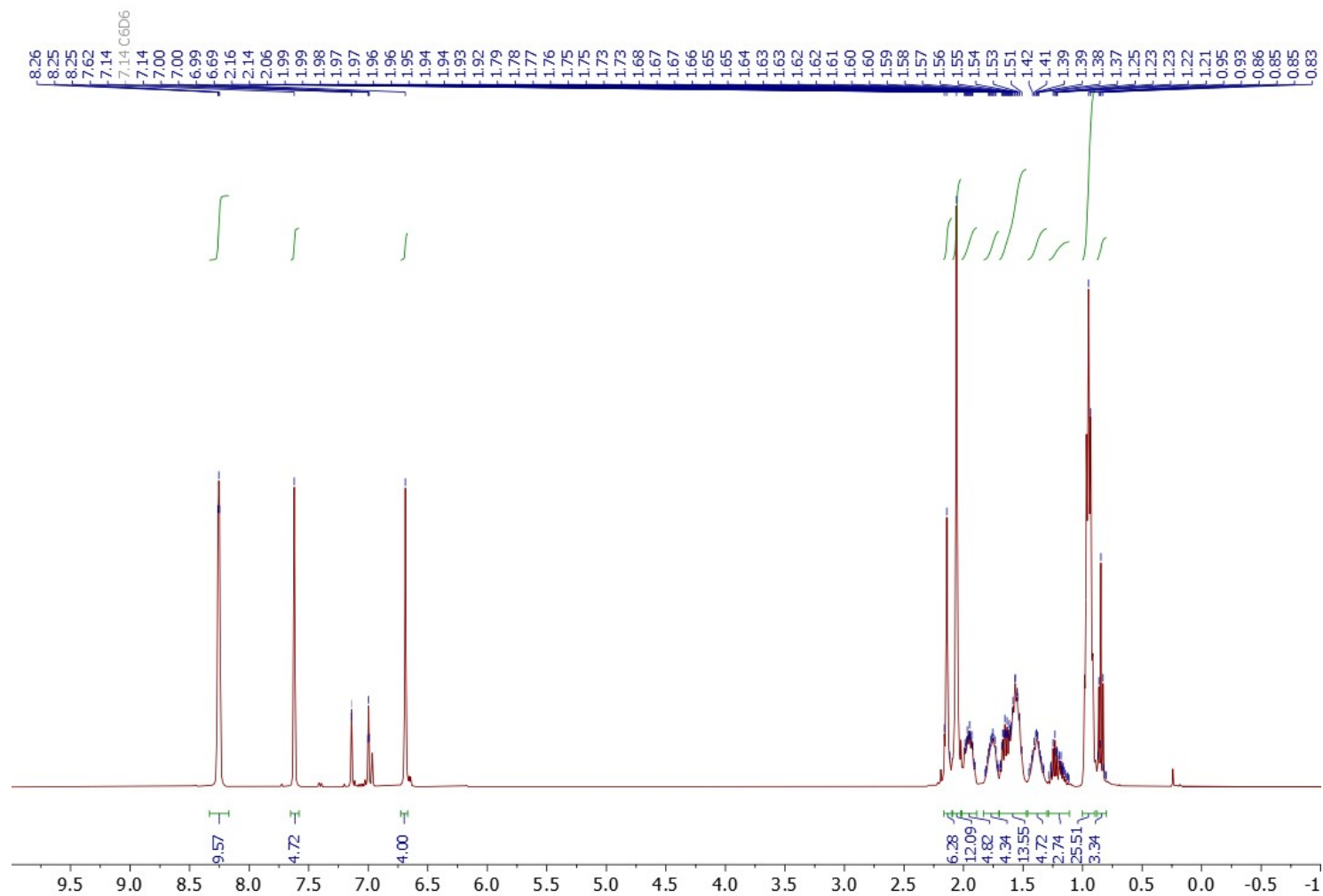


Figure S22. ^{11}B NMR (128 MHz, $\text{C}_6\text{D}_5\text{Cl}$).

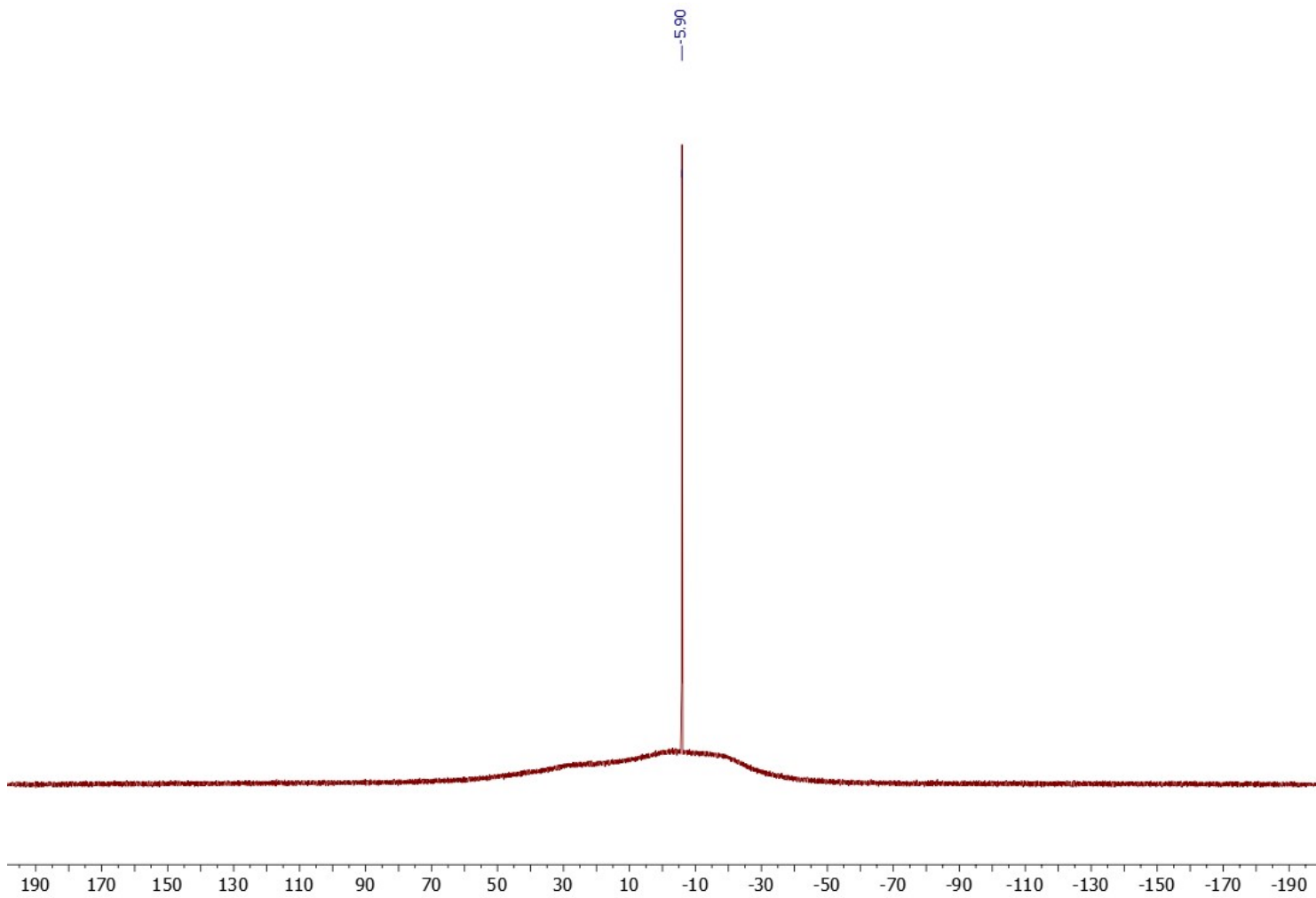


Figure S23. $^{13}\text{C}\{^1\text{H}\}$ NMR (100 MHz, $\text{C}_6\text{D}_5\text{Cl}$).

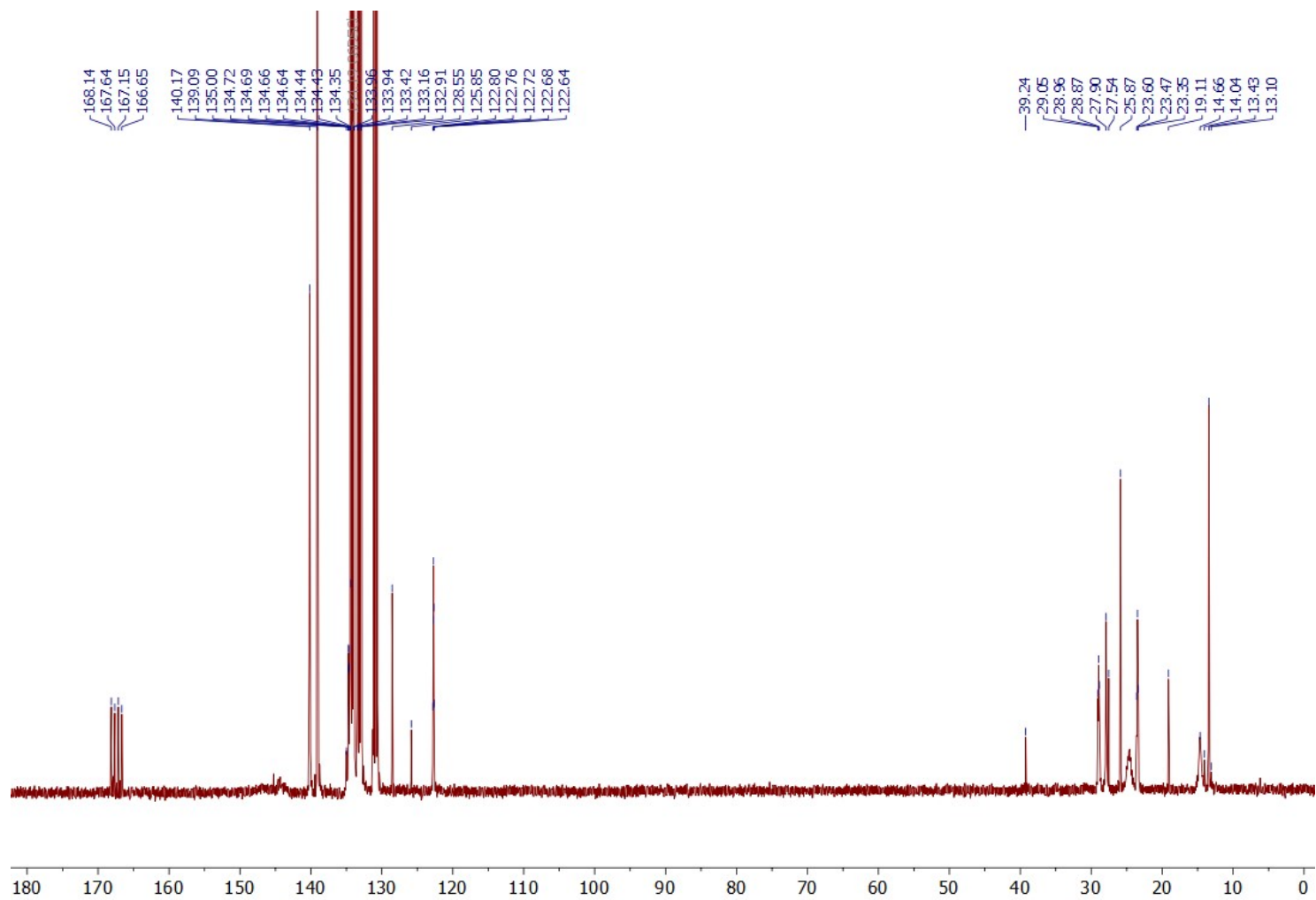


Figure S24. ^{19}F NMR (376 MHz, C_6D_6).

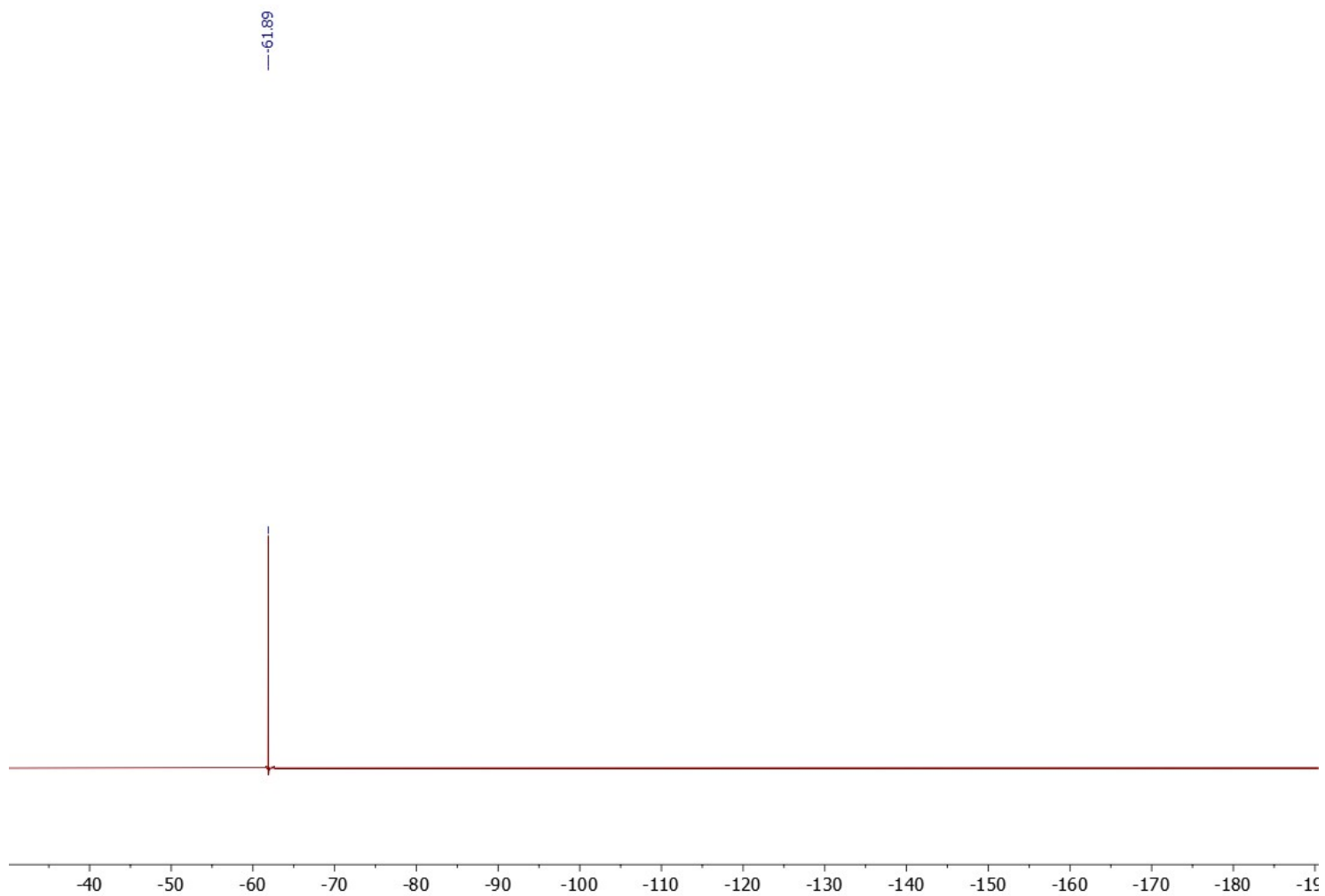


Figure S25. ^{31}P NMR (162 MHz, $\text{C}_6\text{D}_5\text{Cl}$).

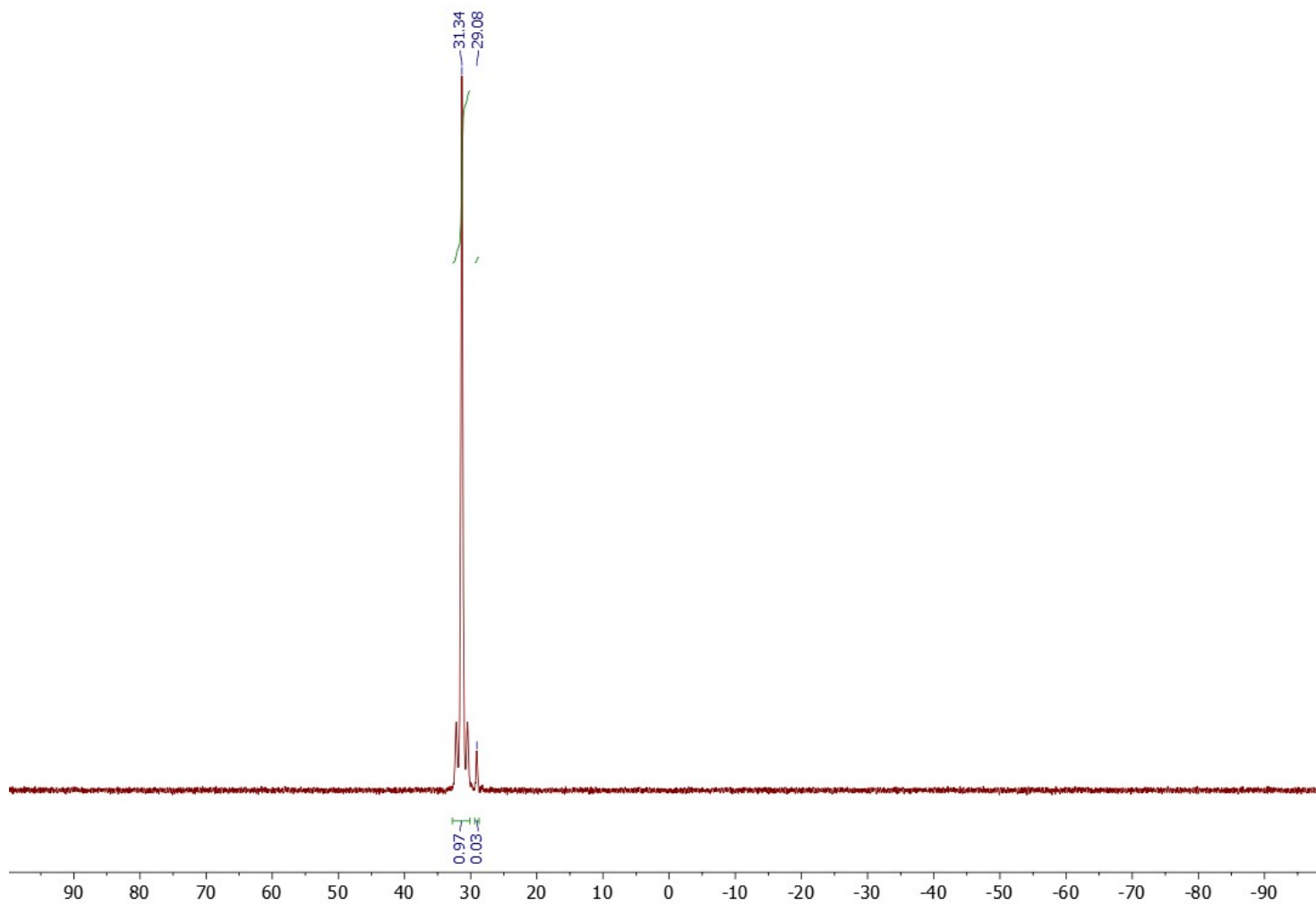
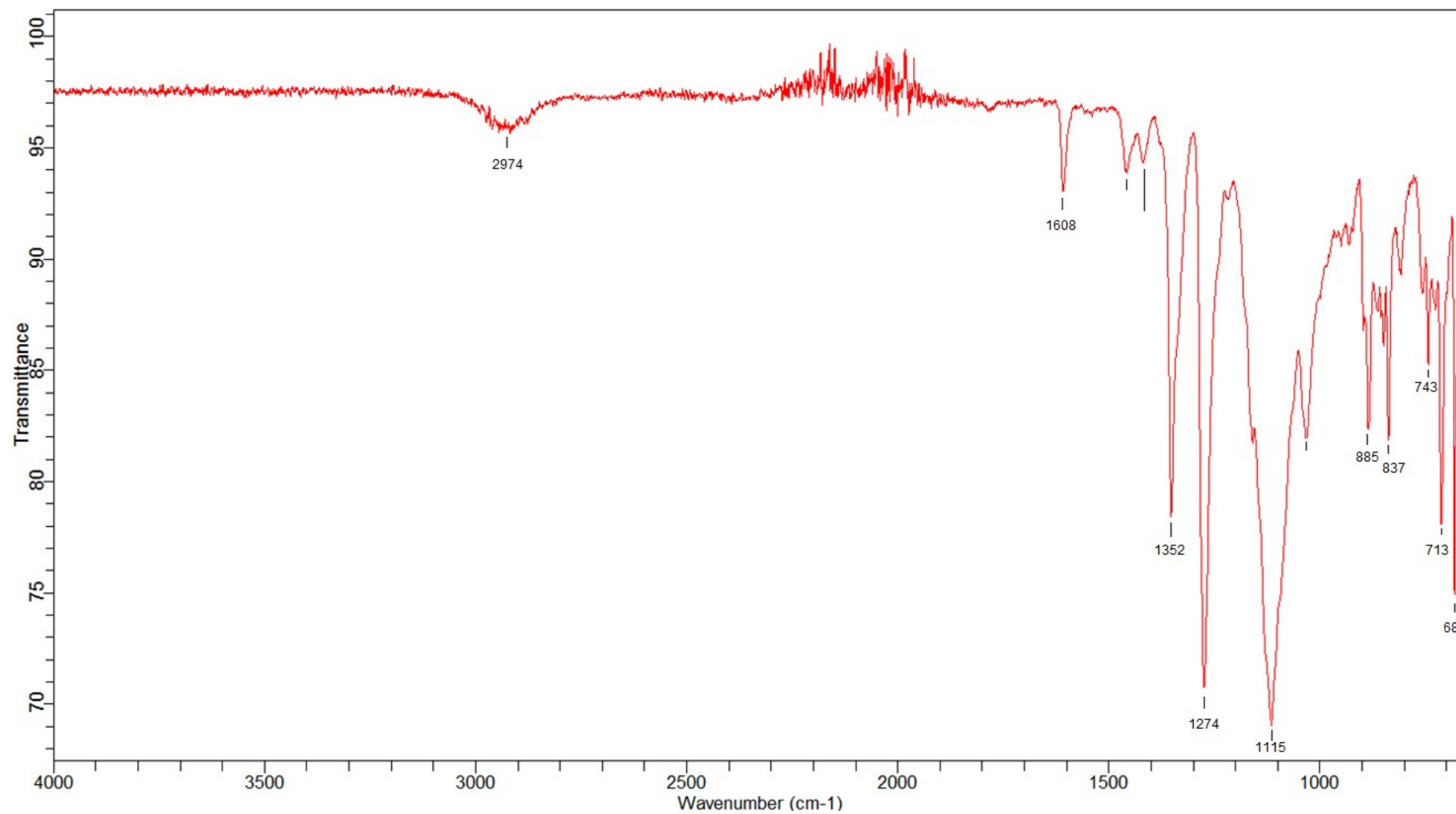


Figure S26. FT-IR (ATR, 400–4000 cm^{-1} range).



III.2. $[\text{W}(\text{CITl})\{\text{N}_2\text{B}(\text{C}_6\text{F}_5)_2\}(\text{dppe})_2] ([3^{\text{Ph}}\text{-Tl}]\text{BAr}^{\text{F}}_4)$

Figure S27. ^1H NMR (400 MHz, C_6D_6).

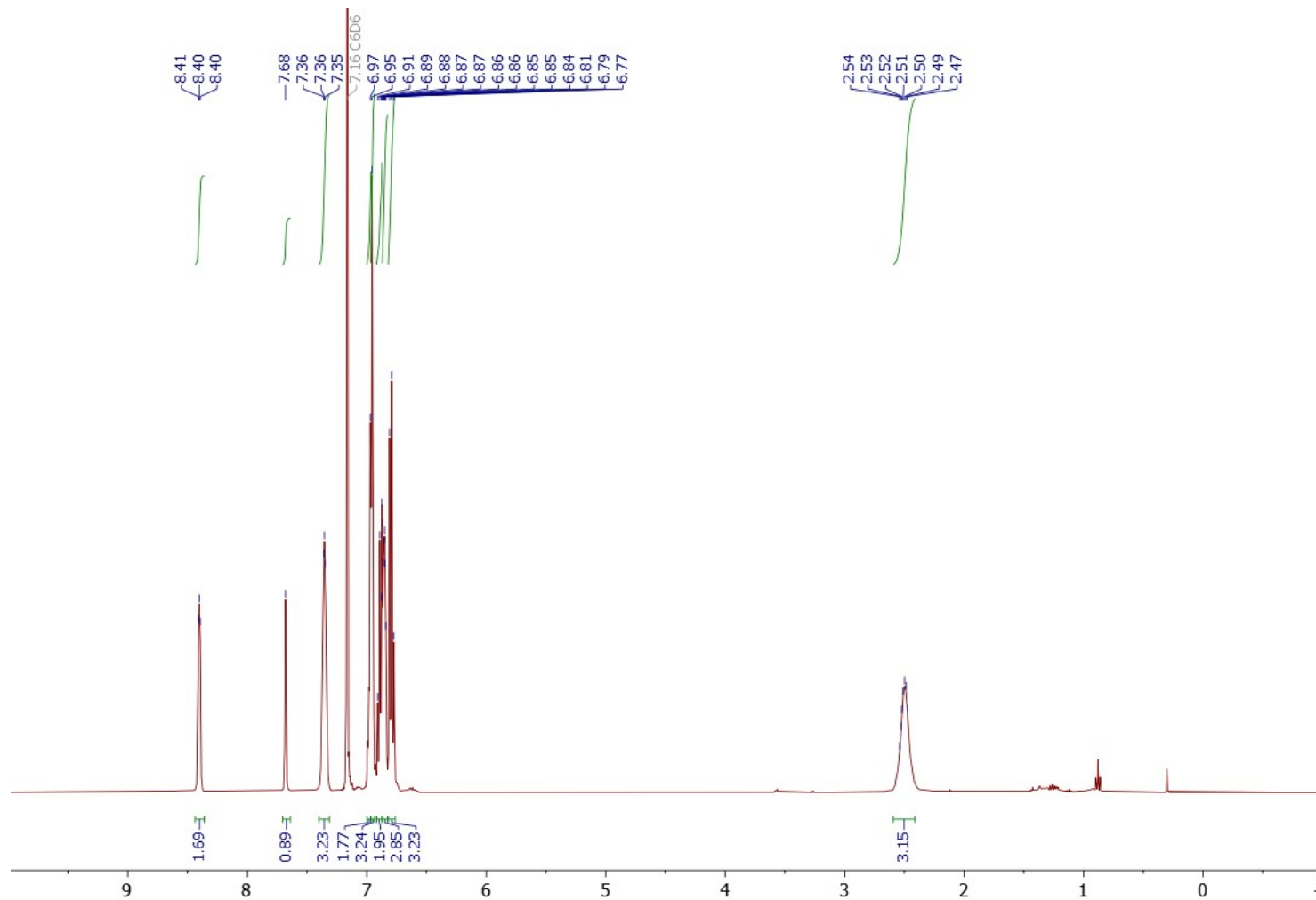


Figure S28. ^1H NMR (400 MHz, $\text{C}_6\text{D}_5\text{Cl}$).

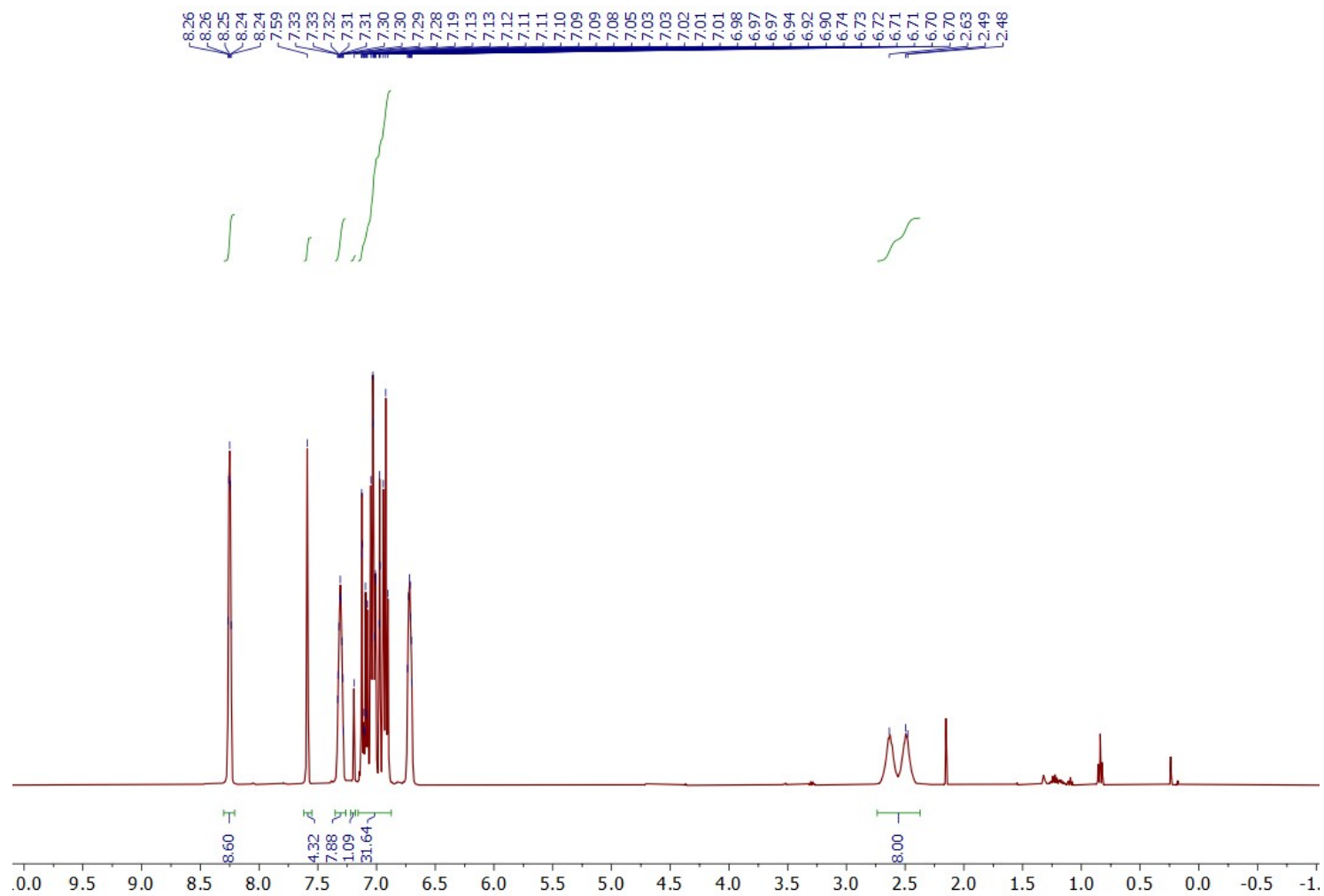


Figure S29. ^{11}B NMR (128 MHz, C_6D_6).

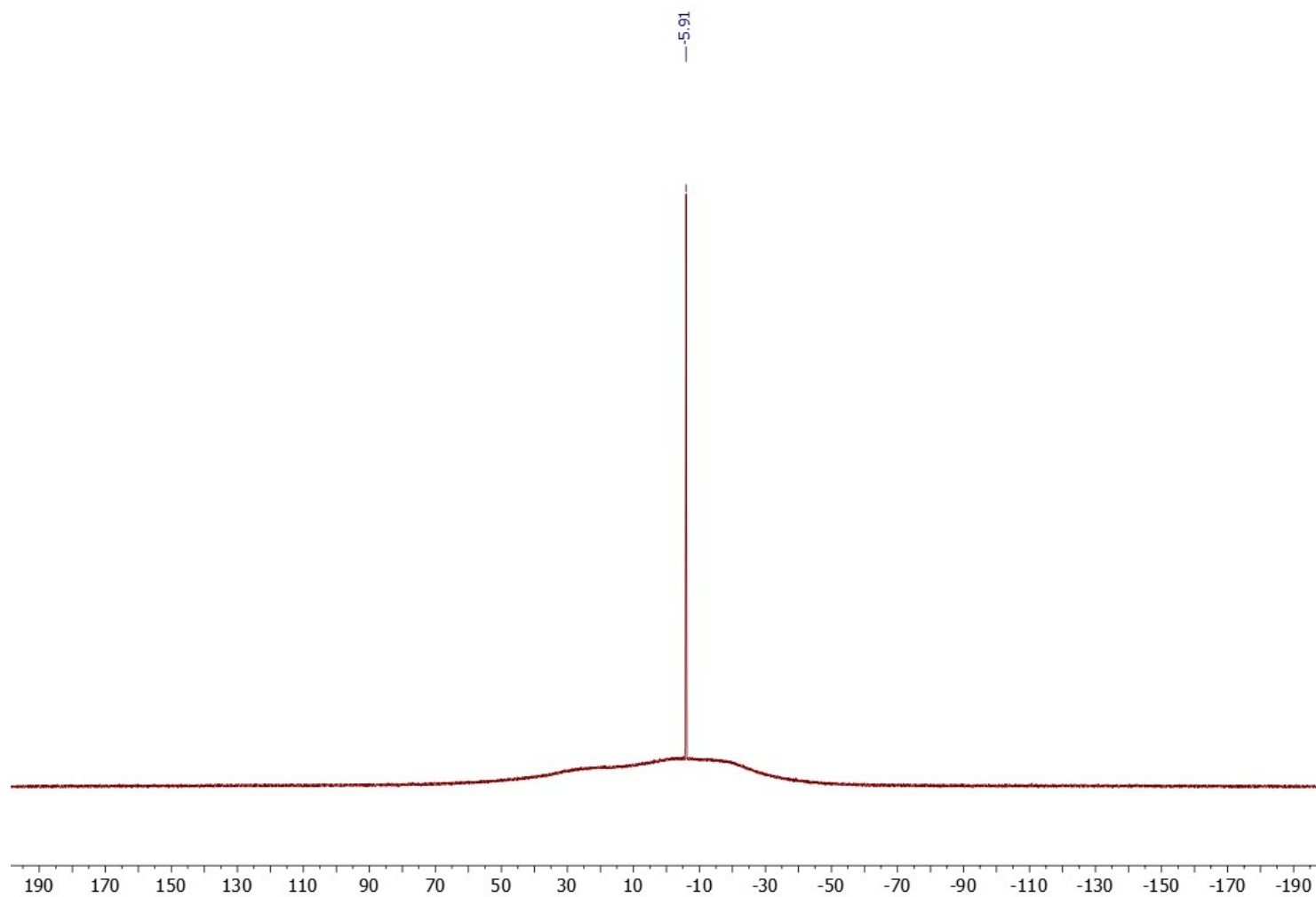


Figure S30. $^{13}\text{C}\{^1\text{H}\}$ NMR (100 MHz, C_6D_6).

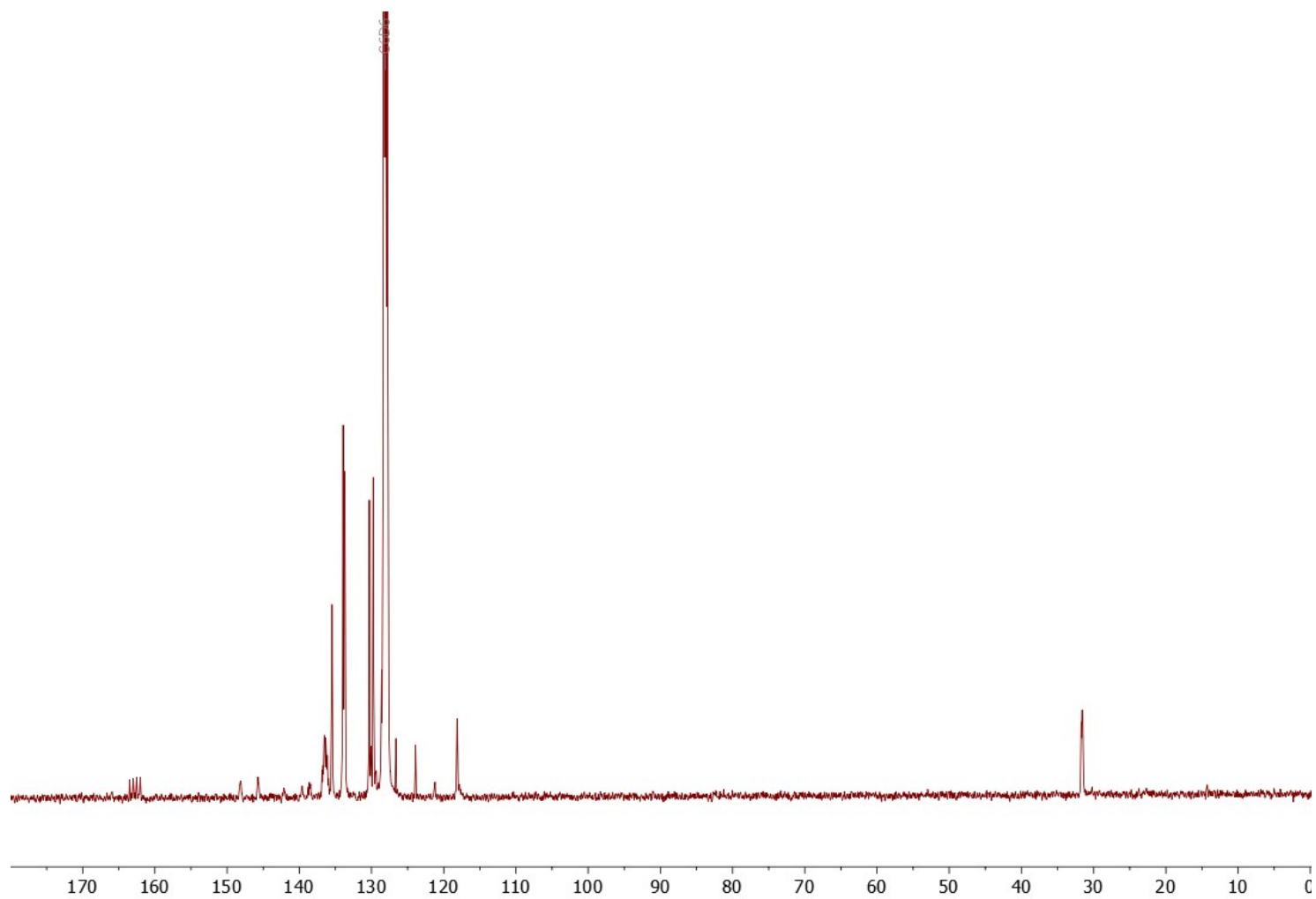


Figure S31. ^{19}F NMR (376 MHz, C_6D_6).

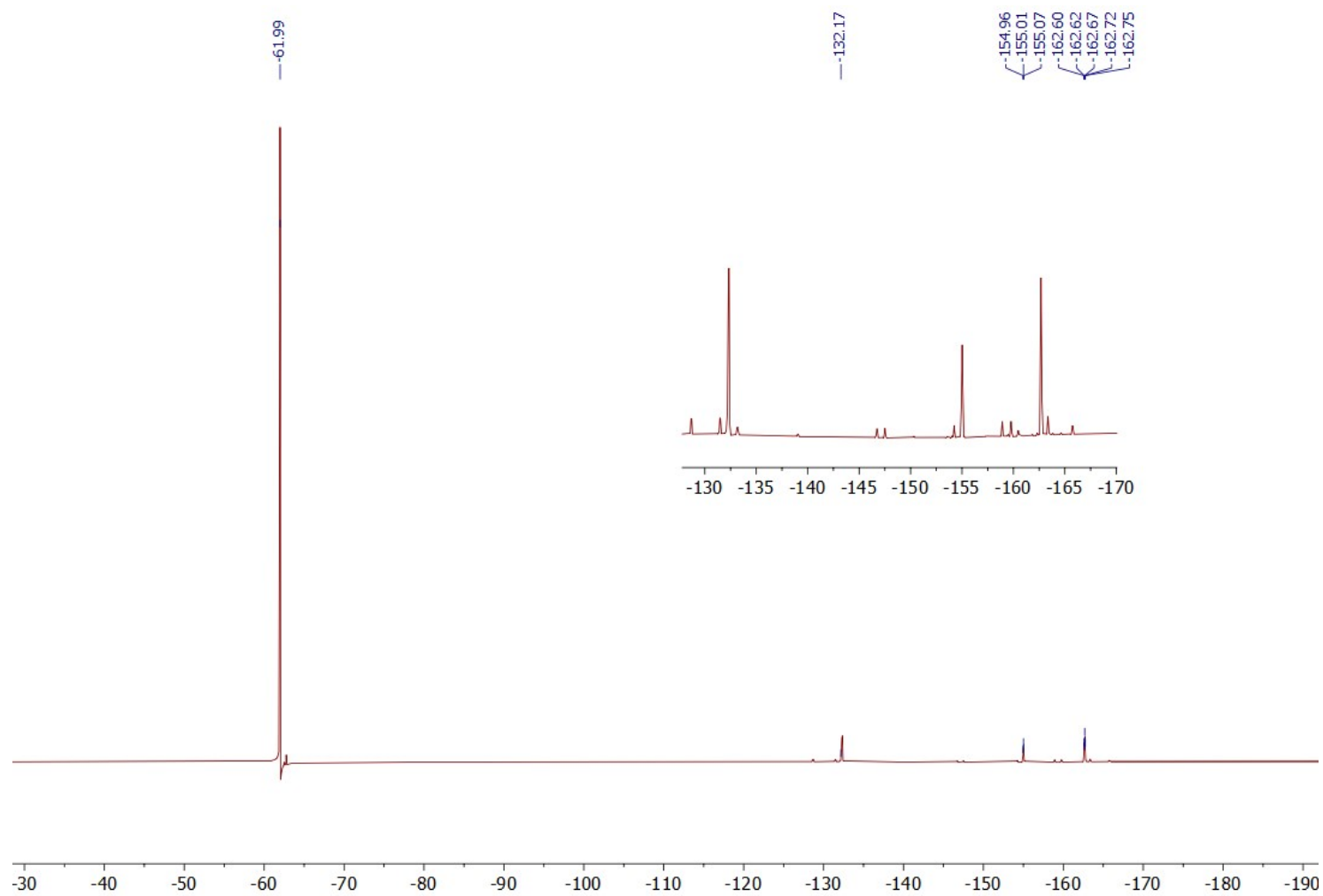


Figure S32. ^{31}P NMR (162 MHz, C_6D_6).

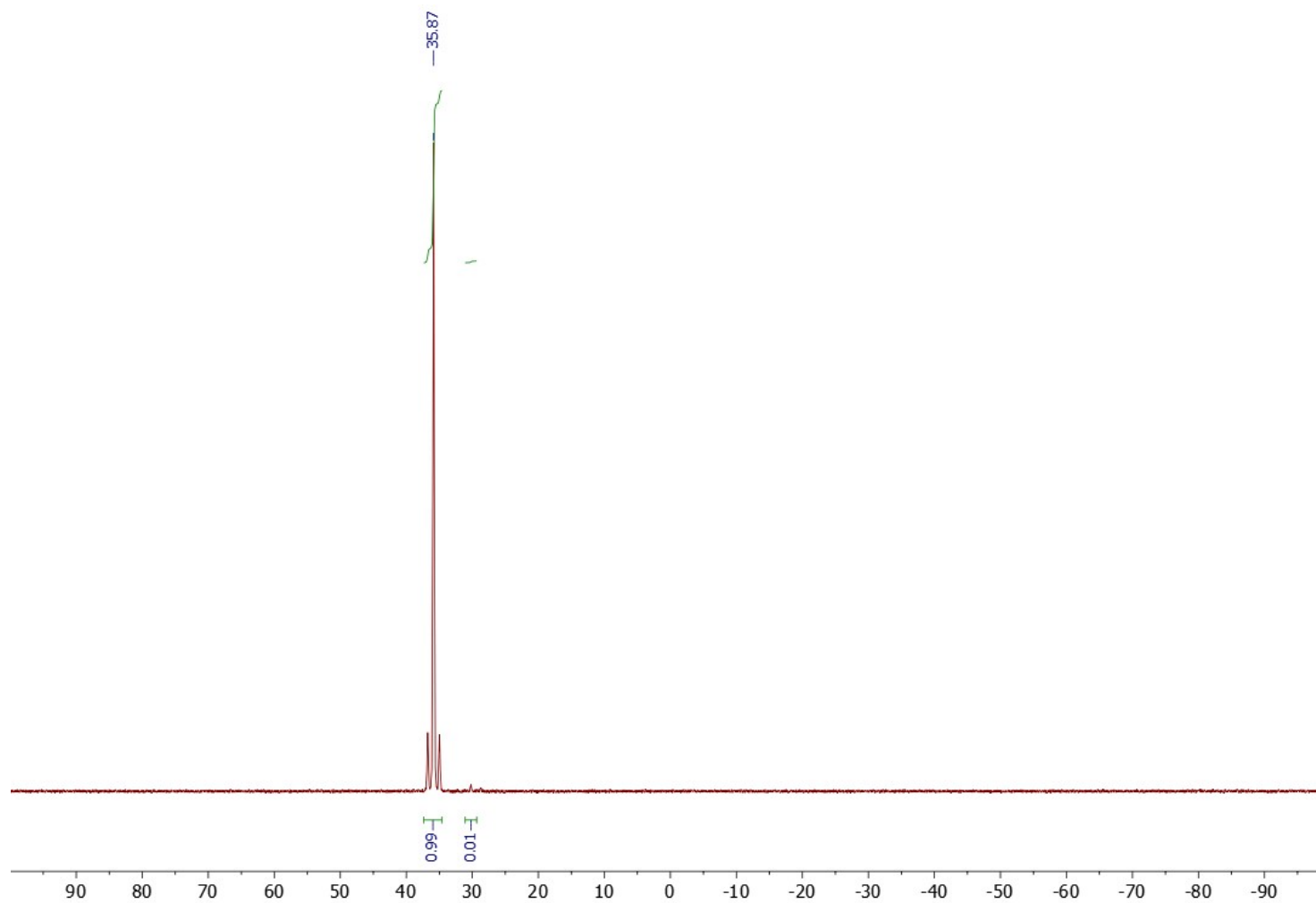
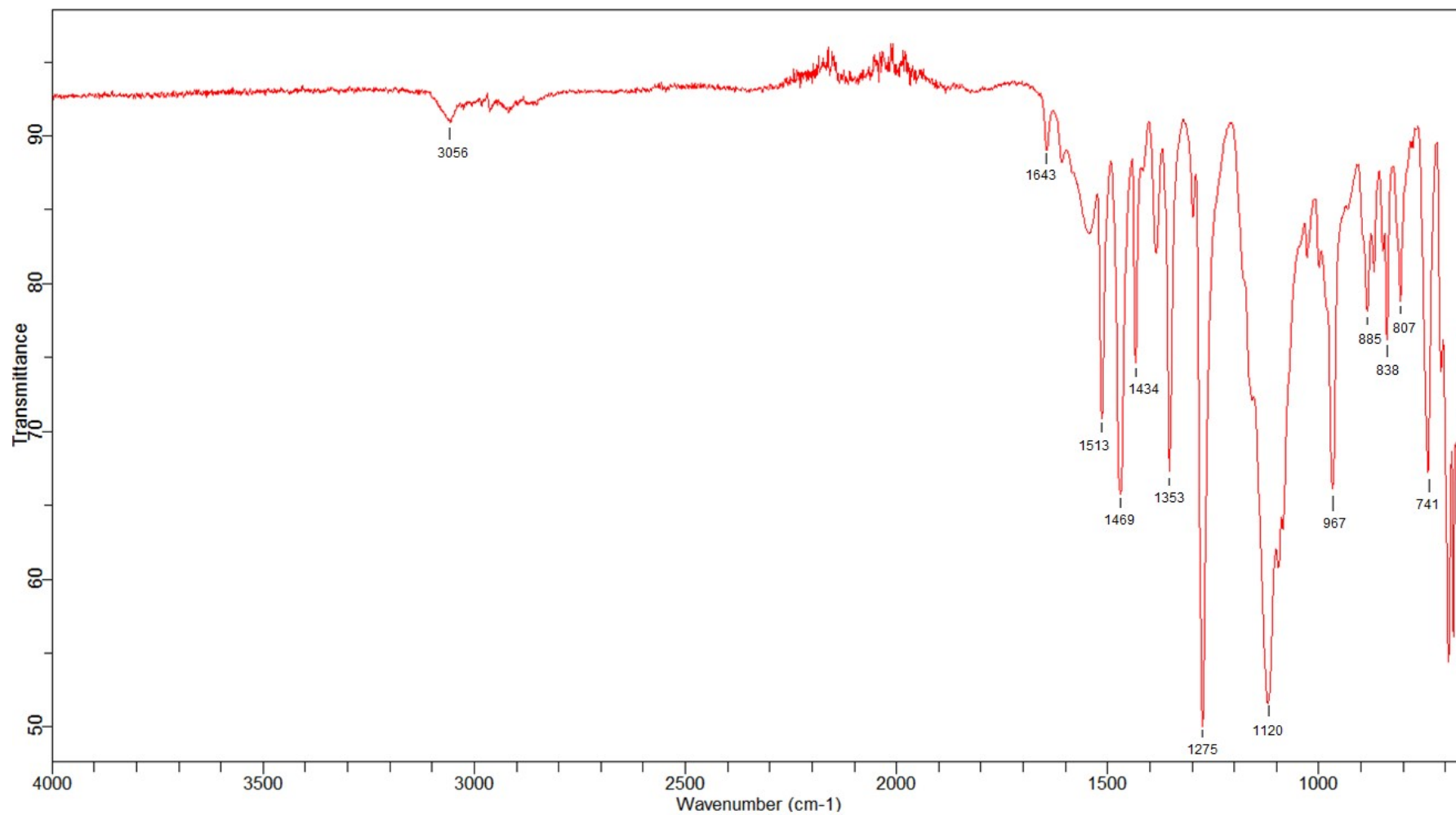


Figure S33. FT-IR (ATR, 400–4000 cm^{-1} range).



IV. Crystallographic data

IV.1. Data collection and refinement

Data for compounds **2^{Ph}**, **2^{Et}**, **3^{Ph}**, **3^{Et}**, [**2^{Et}·TI**]BAr^F₄ and [**3^{Ph}·TI**]BAr^F₄ were collected at low temperature (100 K) on a Bruker Kappa Apex II diffractometer using a Mo-Ka radiation ($\lambda = 0.71073\text{\AA}$) micro-source and equipped with an Oxford Cryosystems Cooler Device. The structures have been solved by Direct Methods and refined by means of least-squares procedures using the SHELXS97^[S7] program included in the softwares package WinGX version 1.63^[S8] or with the aid of the software package Crystal^[S9]. The Atomic Scattering Factors were taken from International tables for X-Ray Crystallography^[S10]. Hydrogen atoms were placed geometrically and refined using a riding model. All non-hydrogens atoms were anisotropically refined. Drawing of molecules in the following figures were performed with the program Mercury^[S11] with 30% probability displacement ellipsoids for non-hydrogen atoms. The crystal structures have been deposited at the Cambridge Crystallographic Data Centre and allocated the deposition numbers CCDC 2114361–2114366 and 2122445.

IV.1.X-Ray analysis of 2^{Ph}

Figure S34. X-ray crystal structure of 2^{Ph}, with ellipsoids set at the 30% probability level; hydrogen atoms omitted for clarity.

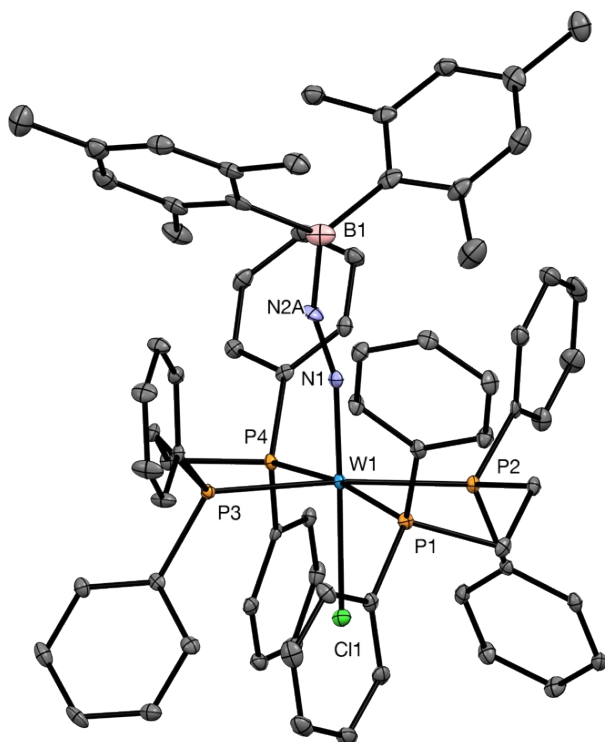


Table S1. Crystallographic data for 2^{Ph}.

Crystal Data	
Chemical formula	C ₇₀ H ₇₀ BClN ₂ P ₄ W
M _r	1293.26
Crystal system, space group	Triclinic, P-1
Temperature (K)	100 K
a, b, c (Å)	13.5795 (6), 18.9959 (8), 24.5911 (10)
α, β, γ (°)	85.873 (1), 78.351 (1), 89.176 (1)
V (Å ³)	6196.6 (5)
Z	4
Radiation type	Mo Kα radiation, λ = 0.71073 Å
μ (mm ⁻¹)	2.05
Crystal size (mm)	0.15 × 0.08 × 0.02
Data collection	
Diffractometer	Bruker Kappa APEX II diffractometer
Absorption correction	Multi-scan [c.f. r.h. blessing, <i>acta cryst.</i> (1995), a51, 33-38]
T _{min} , T _{max}	0.668, 0.746
No. of measured, independent and observed [I > 2σ(I)] reflections	138108, 21899, 16338
R _{int}	0.092
θ _{max} (°)	25.0
Refinement	
R[F ² > 2σ(F ²)], wR(F ²), S	0.031, 0.060, 0.96
No. of reflections	21899
No. of parameters	1438
H-atom treatment	H-atom parameters constrained
Δρ _{max} , Δρ _{min} (e Å ⁻³)	0.65, -0.96

IV.2.X-Ray analysis of 2^{Et}

Figure S35. X-ray crystal structure of 2^{Et}, with ellipsoids set at the 30% probability level; hydrogen atoms omitted for clarity.

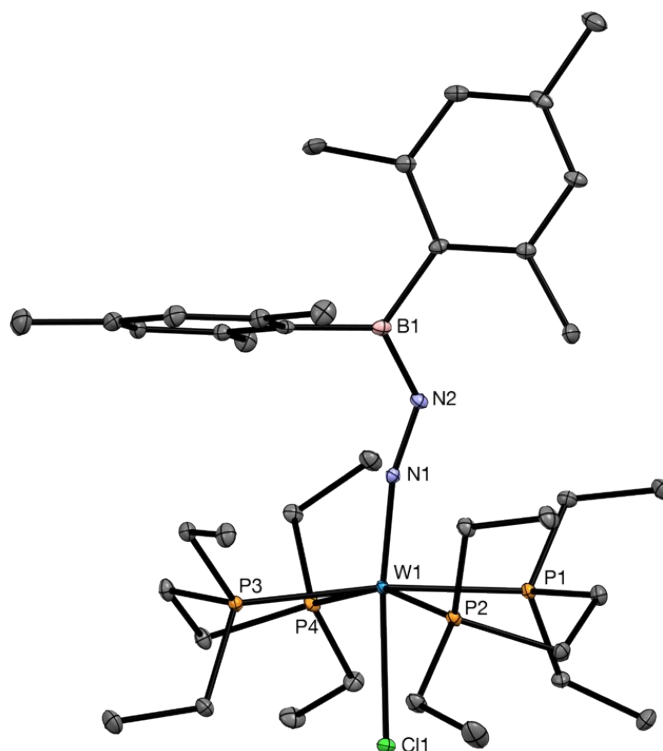


Table S2. Crystallographic data for 2^{Et}.

Crystal data	
Chemical formula	C ₃₂ H ₆₉ BCIN ₂ P ₄ W
M _r	907.99
Crystal system, space group	Monoclinic, C2/c
Temperature (K)	100 K
a, b, c (Å)	31.524 (2), 13.0407 (8), 21.6455 (14)
α, β, γ (°)	91.897 (3)
V (Å ³)	8893.6 (10)
Z	8
Radiation type	Mo Kα radiation, λ = 0.71073 Å
μ (mm ⁻¹)	2.82
Crystal size (mm)	0.18 × 0.10 × 0.03
Data collection	
Diffractometer	Bruker Kappa APEX II diffractometer
Absorption correction	multi-scan SADABS (Siemens, 1996)
T _{min} , T _{max}	0.82, 0.92
No. of measured, independent and observed [I > 2σ(I)] reflections	149547, 16194, 12199
R _{int}	0.102
θ _{max} (°)	33.2
Refinement	
R[F ² > 2σ(F ²)], wR(F ²), S	0.035, 0.073, 0.98
No. of reflections	16186
No. of parameters	424
H-atom treatment	H-atom parameters constrained
Δρ _{max} , Δρ _{min} (e Å ⁻³)	2.47, -2.29

IV.3.X-Ray analysis of 3^{Ph}

Figure S36. X-ray crystal structure of 3^{Ph}, with ellipsoids set at the 30% probability level; hydrogen atoms omitted for clarity.

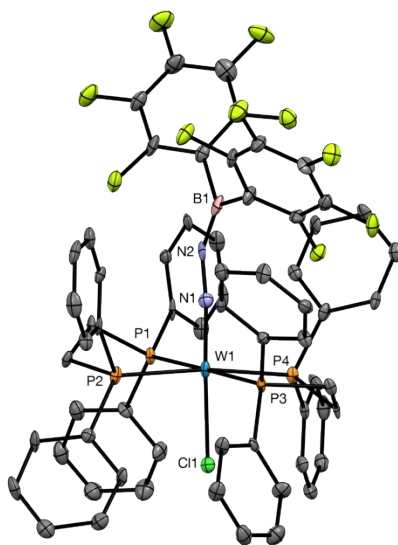


Table S3. Crystallographic data for 3^{Et}.

Crystal data	
C ₇₉ H ₆₁ BCl ₂ F ₁₀ N ₂ OP ₄ W	
<i>M_r</i> = 1633.73	<i>D_x</i> = 1.564 Mg m ⁻³
Monoclinic, C2/c	Melting point:
Hall symbol: -C 2yc	Mo K α radiation, λ = 0.71073 Å
<i>a</i> = 31.319 (5) Å	Cell parameters from 32.49 reflections
<i>b</i> = 23.807 (4) Å	θ = 2.6–20.0°
<i>c</i> = 19.028 (4) Å	μ = 1.91 mm ⁻¹
β = 102.001 (5)°	<i>T</i> = 103 K
<i>V</i> = 13877 (4) Å ³	Platelet, light yellow
<i>Z</i> = 8	0.11 × 0.08 × 0.02 mm
<i>F</i> (000) = 6560	
Data collection	
Bruker Kappa Apex2 diffractometer	6361 reflections with <i>I</i> > 2 σ (<i>I</i>)
Radiation source: ?	<i>R</i> _{int} = 0.329
Graphite monochromator	θ_{max} = 24.7°, θ_{min} = 1.1°
φ & ω scans	<i>h</i> = -36 36
Absorption correction: multi-scan	<i>k</i> = -26 28
SADABS (Siemens, 1996)	<i>l</i> = -22 22
<i>T</i> _{min} = 0.542, <i>T</i> _{max} = 0.745	
113592 measured reflections	
11810 independent reflections	
Refinement	
Refinement on <i>F</i> ²	
Least-squares matrix: full	Hydrogen site location: mixed
<i>R</i> [<i>F</i> ² > 2 σ (<i>F</i> ²)] = 0.077	H-atom parameters constrained
<i>wR</i> (<i>F</i> ²) = 0.220	$w = 1/[\sigma^2(F_o^2) + (0.0941P)^2 + 124.3535P]$ where $P = (F_o^2 + 2F_c^2)/3$
<i>S</i> = 1.05	(Δ/σ) _{max} = 0.001
11810 reflections	$\Delta\rho_{\text{max}} = 2.87 \text{ e } \text{Å}^{-3}$
886 parameters	$\Delta\rho_{\text{min}} = -2.83 \text{ e } \text{Å}^{-3}$
37 restraints	Extinction correction: none

IV.4.X-Ray analysis of 3^{Et}

Figure S37. X-ray crystal structure of 3^{Et}, with ellipsoids set at the 30% probability level; hydrogen atoms omitted for clarity.

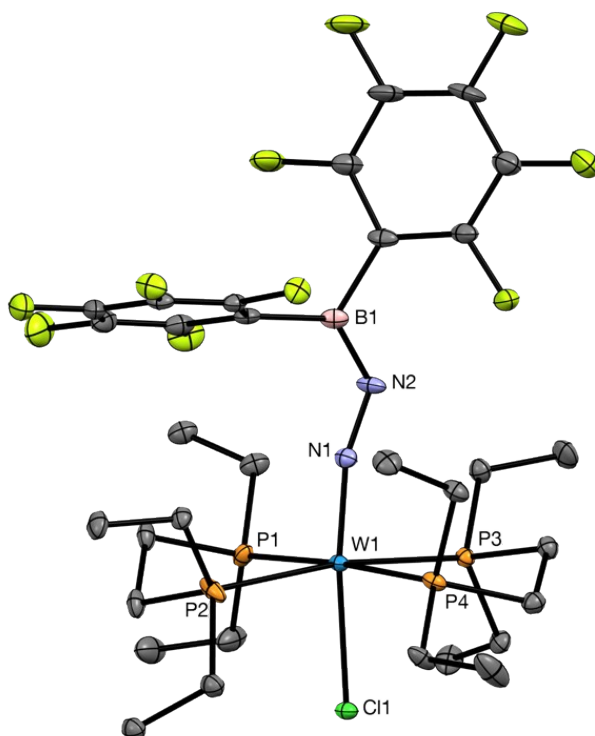


Table S4. Crystallographic data for 3^{Et}.

Crystal data	
Chemical formula	C ₃₂ H ₄₈ BClF ₁₀ N ₂ P ₄ W
M _r	1004.71
Crystal system, space group	Monoclinic, <i>P</i> ₂ ₁ / <i>n</i>
Temperature (K)	110 K
a, b, c (Å)	11.8464 (4), 13.1720 (3), 27.4046 (4)
α, β, γ (°)	99.148 (3)
V (Å ³)	4221.84 (19)
Z	4
Radiation type	Mo Kα radiation, λ = 0.71073 Å
μ (mm ⁻¹)	3.02
Crystal size (mm)	0.10 × 0.05 × 0.02
Data collection	
Diffractometer	Bruker Kappa APEX II diffractometer
Absorption correction	multi-scan c.f. r.h. blessing, acta cryst. (1995), a51, 33-38
T _{min} , T _{max}	0.665, 0.746
No. of measured, independent and observed [I > 2σ(I)] reflections	188070, 21208, 16637
R _{int}	0.066
θ _{max} (°)	25.7
Refinement	
R[F ² > 2σ(F ²)], wR(F ²), S	0.028, 0.067, 1.05
No. of reflections	7963
No. of parameters	472
H-atom treatment	H-atom parameters constrained
Δρ _{max} , Δρ _{min} (e Å ⁻³)	1.57, -1.22

IV.5.X-Ray analysis of $[\text{WCl}_2(\text{depe})_2]\text{BAr}^{\text{F}_4}$

Figure S38. X-ray crystal structure of $[\text{WCl}_2(\text{depe})_2]\text{BAr}^{\text{F}_4}$, with ellipsoids set at the 30% probability level; hydrogen atoms omitted for clarity.

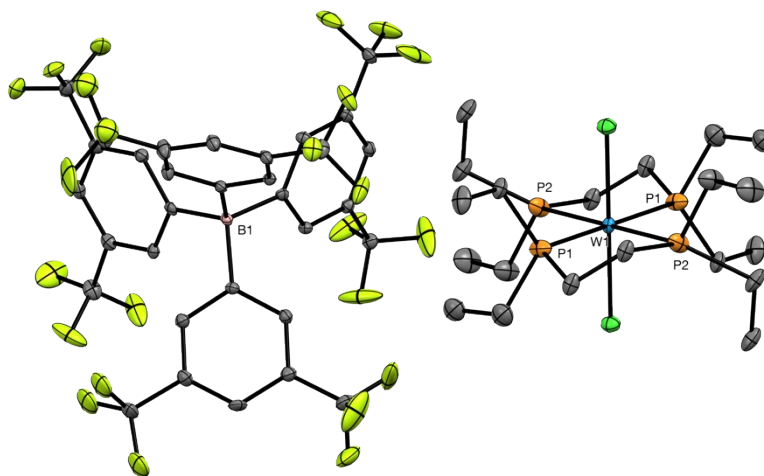


Table S5. Crystallographic data for $[\text{WCl}_2(\text{depe})_2]\text{BAr}^{\text{F}_4}$.

Crystal data	
$\text{C}_{32}\text{H}_{12}\text{BF}_{24} \cdot \text{C}_{20}\text{H}_{48}\text{Cl}_2\text{P}_4\text{W}$	$F(000) = 1622$
$M_r = 1530.43$	
Triclinic, $P -1$	$D_x = 1.508 \text{ Mg m}^{-3}$
Hall symbol: $-P 1$	
$a = 12.8472 (1) \text{ \AA}$	Mo $K\alpha$ radiation, $\lambda = 0.71073 \text{ \AA}$
$b = 14.4461 (1) \text{ \AA}$	Cell parameters from 9988 reflections
$c = 19.3710 (1) \text{ \AA}$	$\theta = 2.5\text{--}29.3^\circ$
$\alpha = 108.898 (4)^\circ$	$\mu = 1.99 \text{ mm}^{-1}$
$\beta = 94.296 (5)^\circ$	$T = 110 \text{ K}$
$\gamma = 94.608 (5)^\circ$	Plate, orange
$V = 3370.84 (9) \text{ \AA}^3$	$0.16 \times 0.11 \times 0.03 \text{ mm}$
$Z = 2$	
Data collection	
Bruker Kappa APEX II diffractometer	9236 reflections with $I > 2\sigma(I)$
Radiation source: Mo micro-focus	$R_{\text{int}} = 0.056$
Graphite monochromator	$\theta_{\text{max}} = 24.7^\circ$, $\theta_{\text{min}} = 1.1^\circ$
ω - ϕ scans	$h = -15 \ 15$
Absorption correction: multi-scan [c.f. r.h. blessing, acta cryst. (1995), a51, 33-38]	$k = -16 \ 16$
$T_{\text{min}} = 0.657$, $T_{\text{max}} = 0.747$	$l = -22 \ 22$
66473 measured reflections	Standard reflections: 0
11372 independent reflections	
Refinement	
Refinement on F^2	
Least-squares matrix: full	Hydrogen site location: inferred from neighbouring sites
$R[F^2 > 2\sigma(F^2)] = 0.041$	H-atom parameters constrained
$wR(F^2) = 0.121$	$w = 1/[\sigma^2(F_o^2) + (0.0654P)^2 + 12.3648P]$ where $P = (F_o^2 + 2F_c^2)/3$
$S = 1.06$	$(\Delta/\sigma)_{\text{max}} = 0.039$
11372 reflections	$\Delta\rho_{\text{max}} = 1.66 \text{ e \AA}^{-3}$
769 parameters	$\Delta\rho_{\text{min}} = -1.04 \text{ e \AA}^{-3}$
9 restraints	Extinction correction: none

IV.6.X-Ray analysis of [3^{Ph}·Ti]BARF₄

Figure S39. X-ray crystal structure of [3^{Ph}·Ti]BARF₄, with ellipsoids set at the 30% probability level; hydrogen atoms omitted for clarity.

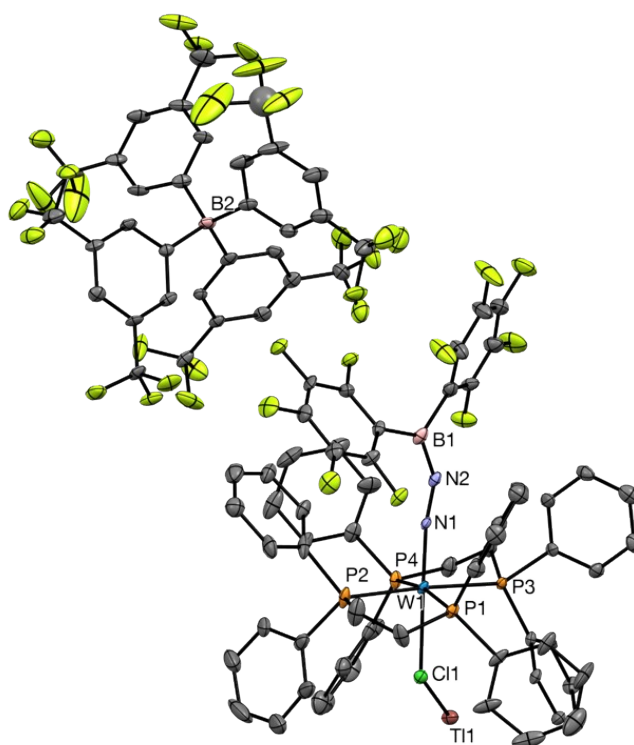


Table S6. Crystallographic data for [3^{Ph}·Ti]BARF₄.

Crystal data	
Chemical formula	C ₁₀₅ H ₆₅ B ₂ ClF ₃₄ N ₂ P ₄ TiW
M _r	2573.84
Crystal system, space group	Triclinic, P-1
Temperature (K)	100 K
a, b, c (Å)	16.7376 (8), 17.7790 (11), 20.2892 (17)
α, β, γ (°)	93.001 (5), 96.278(6), 92.960(4)
V (Å ³)	5983.2 (7)
Z	2
Radiation type	Mo Kα radiation, λ = 0.71073 Å
μ (mm ⁻¹)	2.48
Crystal size (mm)	0.15 × 0.11 × 0.02
Data collection	
Diffractometer	Bruker Kappa APEX II diffractometer
Absorption correction	multi-scan <i>SADABS</i> (Siemens, 1996)
T _{min} , T _{max}	0.86, 0.95
No. of measured, independent and observed [I > 2σ(I)] reflections	20983, 20983, 14076
R _{int}	0.000
θ _{max} (°)	25.0
Refinement	
R[F ² > 2σ(F ²)], wR(F ²), S	0.05, 0.055, 1.09
No. of reflections	12643
No. of parameters	1346
H-atom treatment	H-atom parameters constrained
Δρ _{max} , Δρ _{min} (e Å ⁻³)	1.19, -1.16

IV.7.X-Ray analysis of [2^{Et}-Ti]BAr^F₄

Figure S40. X-ray crystal structure of [2^{Et}-Ti]BAr^F₄, with ellipsoids set at the 30% probability level; hydrogen atoms omitted for clarity.

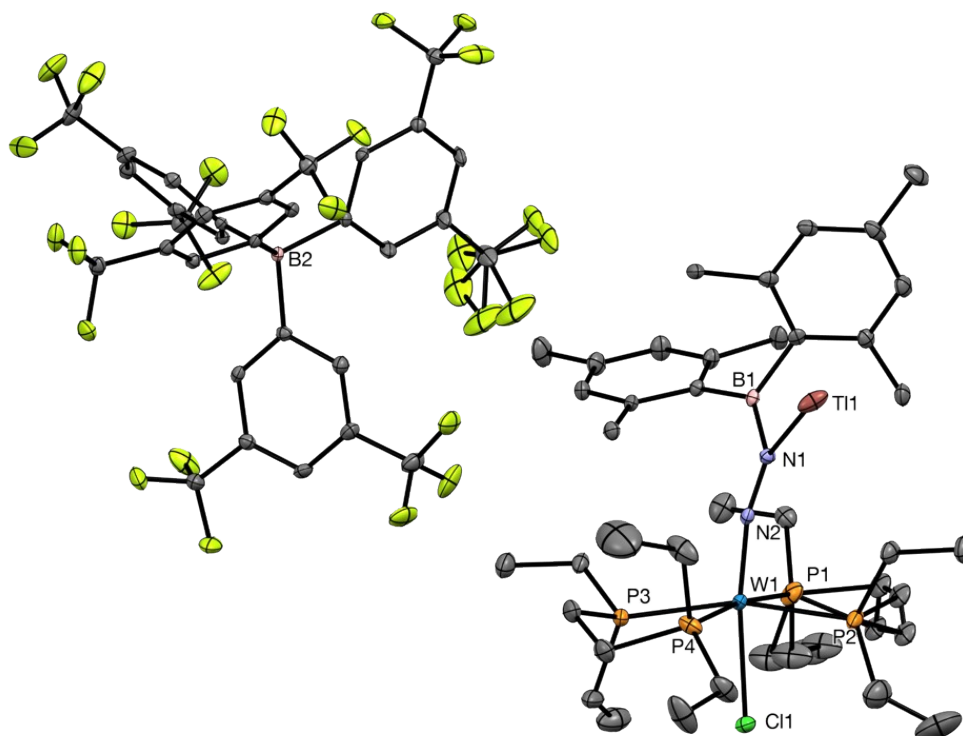


Table S7. Crystallographic data for [2^{Et}-Ti]BAr^F₄.

Crystal data	
Chemical formula	C ₇₀ H ₈₂ B ₂ ClF ₂₄ N ₂ P ₄ TiW
M _r	1976.58
Crystal system, space group	Monoclinic, P 2 ₁ /c
Temperature (K)	110 K
a, b, c (Å)	19.4938 (4), 20.5553 (5), 19.9296 (4)
α, β, γ (°)	106.853 (3)
V (Å ³)	7642.85 (14)
Z	4
Radiation type	Mo Kα radiation, λ = 0.71073 Å
μ (mm ⁻¹)	3.829
Crystal size (mm)	0.12 × 0.12 × 0.14
Data collection	
Diffractometer	Bruker Kappa APEX II diffractometer
Absorption correction	multi-scan SADABS (Siemens, 1996)
T _{min} , T _{max}	0.56, 0.63
No. of measured, independent and observed [I > -3σ(I)] reflections	214287, 23419, 14999
R _{int}	0.0883
θ _{max} (°)	30.57
Refinement	
R[F ² > 2σ(F ²)], wR(F ²), S	0.061, 0.117, 0.99
No. of reflections	9384
No. of parameters	940
H-atom treatment	H-atom parameters constrained
Δρ _{max} , Δρ _{min} (e Å ⁻³)	6.89, -6.22

V. References

- [S1] R. K. Harris, E. D. Becker, S. M. Cabral de Menezes, R. Goodfellow and P. Granger, *Pure Appl. Chem.*, 2001, **73**, 1795–1818.
- [S2] J. R. Dilworth and R. L. Richards, *Inorg. Synth.*, 1990, **28**, 33–43.
- [S3] A. C. Filippou, G. Schnakenburg, A. I. Philippopoulos and N. Weidemann, *Angew. Chem. Int. Ed.*, 2005, **44**, 5979–5985.
- [S4] D. J. Parks, W. E. Piers and G. P. A. Yap, *Organometallics*, 1998, **17**, 5492–5503.
- [S5] A. Sundararaman and F. Jäkle, *J. Organomet. Chem.*, 2003, **681**, 134–142.
- [S6] J. Cullinane, A. Jolleys and F. S. Mair, *Dalton Trans.*, 2013, **42**, 11971–11975.
- [S7] SHELX97 [Includes SHELXS97, SHELXL97, CIFTAB] - Programs for Crystal Structure Analysis (Release 97-2). G. M. Sheldrick, Institut für Anorganische Chemie der Universität, Tammanstrasse 4, D-3400 Göttingen, Germany, 1998.
- [S8] L. J. Farrugia, *J. Appl. Crystallogr.* 1999, **32**, 837.
- [S9] CRYSTALS version 12: software for guided crystal structure analysis, P. W. Betteridge, J. R. Carruthers, R. I. Cooper, K. Prout and D. J. Watkin, *J. Appl. Cryst.* 2003, **36**, 1487.
- [S10] International Tables for X-Ray Crystallography Vol. IV, Kynoch press, Birmingham, England, 1974.
- [S11] L. J. Farrugia, *J. Appl. Crystallogr.* 1997, **30**, 565.